Nanoscale Advances

ROYAL SOCIETY OF CHEMISTRY

REVIEW

View Article Online
View Journal | View Issue

Cite this: *Nanoscale Adv.*, 2023, **5**, 27

Engineering functional natural polymer-based nanocomposite hydrogels for wound healing

Min Wang,†[a] Zexing Deng, †[b] Yi Guo†[c] and Peng Xu *[a]

Skin injury occurs due to acute trauma, chronic trauma, infection, and surgical intervention, which can result in severe dysfunction and even death in humans. Therefore, clinical intervention is critical for the treatment of skin wounds. One idealized method is to use wound dressings to protect skin wounds and promote wound healing. Among these wound dressings, nanocomposite natural polymer hydrogels (NNPHs) are multifunctional wound dressings for wound healing. The combination of nanomaterials and natural polymer hydrogels avoids the shortcomings of a single component. Moreover, nanomaterials could provide improved antibacterial, anti-inflammatory, antioxidant, stimuli-responsive, electrically conductive and mechanical properties of hydrogels to accelerate wound healing. This review focuses on recent advancements in NNPHs for skin wound healing and repair. Initially, the functions and requirements of NNPHs as wound dressings were introduced. Second, the design, preparation and capacities of representative NNPHs are classified based on their nanomaterial. Third, skin wound repair applications of NNPHs have been summarized based on the types of wounds. Finally, the potential issues of NNPHs are discussed, and future research is proposed to prepare idealized multifunctional NNPHs for skin tissue regeneration.

Received 11th October 2022
Accepted 17th November 2022

DOI: 10.1039/d2na00700b

rsc.li/nanoscale-advances

1. Introduction

Skin serves as the largest organ, protects and covers us from external injury (mechanical, heat, and UV radiation), maintains temperature and moisture, excretes waste from humans and senses stimuli.[1,2] However, both trauma and physiological environment can cause harm to skin tissue, making skin wounds become a common healthcare problem.[3,4] Skin usually exhibits excellent regenerative properties, and normal skin wound healing involves a series of highly ordered processes including hemostasis, inflammation, proliferation, and extracellular matrix (ECM) remodeling,[5–8] as shown in Fig. 1. These four stages of skin wound healing involve interactions among cells, bioactive factors, and ECM.[9–13] However, some of the skin wounds are difficult to heal by themselves on account of infectious, chronic diseases and severe injuries.[14–18] As a result,

[a]*Honghui Hospital, Xi'an Jiaotong University, Xi'an 710000, China. E-mail: sousou369@163.com*

[b]*College of Materials Science and Engineering, Xi'an University of Science and Technology, Xi'an, 710054, China*

[c]*Shaanxi Key Laboratory of Brain Disorders, Shaanxi Key Laboratory of Ischemic Cardiovascular Disease, Institute of Basic and Translational Medicine, Xi'an Medical University, Xi'an, 710021, China*

† M. Wang, Z. Deng, and Y. Guo contributed equally to this paper.

Min Wang received his PhD degree in materials science and engineering under the supervision of Prof. Bo Lei from Xi'an Jiaotong University. He is now working as a post-doctoral researcher at Honghui Hospital, Xi'an Jiaotong University. His research focuses on engineering multifunctional bioactive citric acid-based biomaterials for skin or cartilage tissue engineering.

Zexing Deng received his PhD degree in materials science and engineering under the supervision of Prof. Baolin Guo from Xi'an Jiaotong University. He was also a visiting scholar at the Department of Biologic and Materials Sciences & Prosthodontics, University of Michigan. He is currently investigating conductive hydrogels for biomedical applications, and is also involved in developing biodegradable conductive scaffolds for tissue engineering.

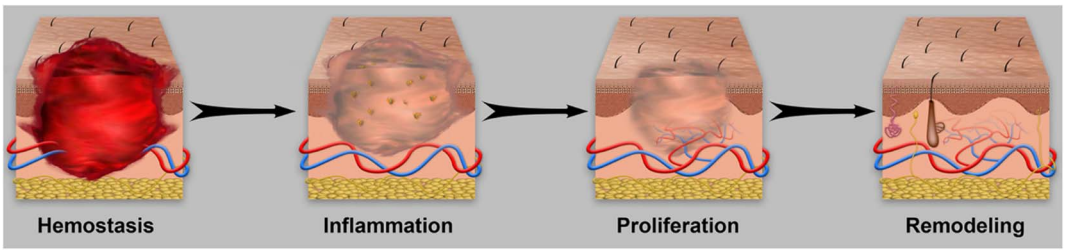

Fig. 1 Illustration of four consecutive stages of wound healing.

skin wound healing has been a major social and financial burden.

The most successful strategies to date are the use of wound dressings or skin substitutes, which can serve as temporary substrates to protect the skin wound surface and provide a therapeutic environment, thereby promoting skin wound healing.[19–21] Consequently, researchers have been developing various types of wound dressings or skin substitutes for many years, and trying to design and fabricate corresponding wound dressings such as nanomaterials,[22,23] microspheres,[24,25] films,[26,27] fibers,[28,29] and hydrogels[30,31] through advanced technology to mimic the microenvironment of skin to promote wound healing. To date, different types of medical products such as HemCon bandage, Tegaderm™ film, and QuikClot bandage have been approved by the Food and Drug Administration (FDA) for hemostasis and wound healing.[32] However, these products have limitations that cannot be ignored, including the difficulty of simultaneous application on external/internal wounds, and the external pressure when applying the product may accompany the secondary injury.[5,32] To address these concerns, hydrogels have been developed by researchers for wound healing due to their good biocompatibility, moisturizing ability, similar structure to ECM and tunable functions.[3] In addition, hydrogels can not only prevent bleeding of external and internal wounds because of their shape adapting ability and hemostatic performance, but also maintain the moisture environment of wounds and absorb exudate to accelerate wound healing and skin tissue regeneration.[32,33]

Hydrogels can be classified based on their source of raw materials, degradability, electrical conductivity, crosslinking method, and stimuli-responsive properties.[34,35] According to the source of raw materials, hydrogels can be divided into natural polymer hydrogels (NPHs), synthetic polymer hydrogels, and

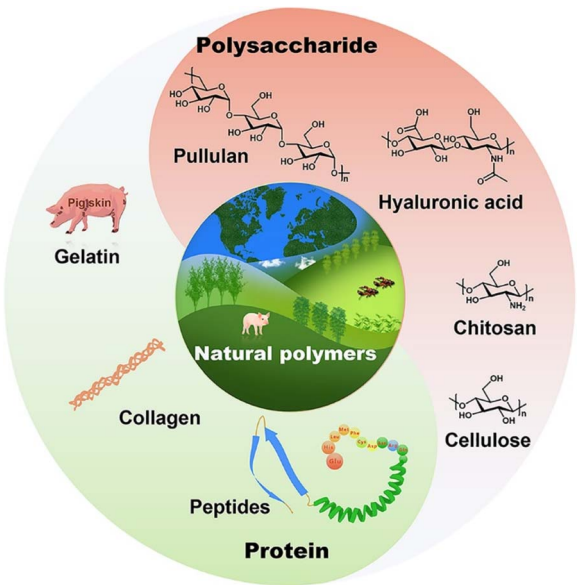

Fig. 2 Illustration of representative natural polymers for building wound dressings.

Yi Guo received her PhD degree in Biomedical Engineering from Xi'an Jiaotong University. She was also a visiting scholar at the Department of Biologic and Materials Sciences & Prosthodontics, University of Michigan. She is now working as a lectorate at the Institute of Basic and Translational Medicine, Xi'an Medical University. Her research mainly focuses on developing bioactive materials for bone or muscle regeneration and cancer therapy.

Prof. Peng Xu is a first-level chief physician, professor, and doctoral supervisor. He is currently the vice president of Honghui Hospital, Xi'an Jiaotong University, president and subject leader of Arthropathy Hospital of Honghui Hospital, Xi'an Jiaotong University, and leading science and technology innovation talent of Shaanxi Province High-level Talents Special Support Program. His research is focused on the treatment of femoral head necrosis and hip-related diseases, osteoarthritis, and cartilage repair.

Table 1 Functions and limitations of typical natural polymers for wound healing

Natural polymers	Functions and advantages	Limitations	Ref.
Hyaluronic acid	Hemostasis; maintaining wound moisture	High price	12, 62, 68, 70, 73 and 74
Gelatin	Hemostasis; promoting cell proliferation	High price and easy degradation	58, 62, 80, 82, 87, 98 and 102
Chitosan	Hemostasis; antibacterial ability; promoting granulation tissue formation	Slow degradation rate	49, 57, 60, 61, 93, 172, 178 and 207
Alginate	Hemostasis; maintaining wound moisture; promoting granulation tissue formation	Low chemical stability and mechanical properties	75, 90, 99, 102, 103 and 210
Dextran	Hemostasis; promoting cell proliferation	—	61, 93, 95 and 96
Cellulose	Hemostasis; antibacterial ability	Slow degradation rate	67, 84 and 203

hybrid hydrogels.[36] Natural polymers coming from animals or plants include gelatin,[37,38] agarose,[39] collagen,[40] polypeptide,[41] pullulan,[42] cellulose,[43] chitosan,[44] and hyaluronic acid[45] and so on, as shown in Fig. 2. Natural polymers can be easily functionalized/modified due to their abundance of $-NH_2$, –OH, and –COOH groups, and generally exhibit good biocompatibility, biodegradability, and gel-forming ability.[46,47] Therefore, many natural polymers such as chitosan, gelatin, hyaluronic acid, alginate and dextran have been investigated for wound healing. Their functions and limitations in wound healing are summarized in Table 1.

However, the disadvantages of weak mechanical properties, poor antioxidant properties, and undesirable stimuli-responsive properties of NPHs greatly block their application in skin wound healing.[48–51] To address these limitations, some functional nanomaterials were incorporated into the hydrogel network to improve antibacterial, antioxidant, and mechanical properties, and electrical conductivity of NPHs as wound dressings to accelerate wound healing.[52,53] In addition, the combination also reduces the limitations of nanomaterials in wound healing, such as causing inflammation on wounds due to a large amount of abrupt release of nanomaterials with a small size.[52,54] Moreover, some nanomaterials can be easily removed due to their undesirable adhesive performance to biological tissue.[55] Representative nanomaterials commonly used in NNPHs for wound healing mainly include carbon-based,[56–62] metal-based,[63–70] MXene-based[71–75] and silicon-based[76–78] nanomaterials, as shown in Table 2 and Fig. 3. Specifically, typical carbon-based nanomaterials involve multi-walled carbon nanotubes (MWCNTs),[79] pluronic F127 (F127)-

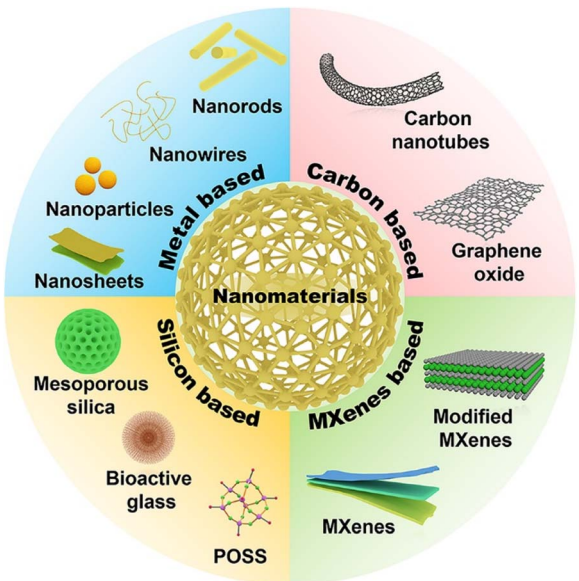

Fig. 3 Classification of NNPHs based on their nanomaterials.

Table 2 Functions and limitations of typical nanomaterials for wound healing

Nanomaterials	Functions and advantages	Limitations	Ref.
Carbon-based	Light-induced antibacterial properties; stimuli-responsive properties; electrical conductivity	Undesirable dispersion	12, 49, 57, 58, 60–62, 80, 82, 83, 172 and 178
Metal-based	Antibacterial properties; stimuli-responsive properties; electrical conductivity	Potential toxicity	67–70, 85, 87, 90, 91, 93, 95–99, 102 and 103
MXenes-based	Good dispersion; stimuli-responsive properties; electrical conductivity	Dangerous chemicals during production	71, 73–75 and 84
Silicon-based	Stability; mechanical reinforcement; cost-effectiveness	Undesirable dispersion and multifunctionality	203, 205, 207, 209 and 210

dispersed MWCNTs,[49] polydopamine (PDA)-coated MWCNTs,[80,81] graphene oxide (GO)[82] and PDA reduced graphene oxide (rGO).[83] MXene-based nanomaterials contain MXene nanosheets,[84] PDA-coated MXene nanosheets,[73] and cerium dioxide (CeO_2)-loaded MXene nanosheets.[71] The representative metal-based nanomaterials include silver (Ag) nanoparticles,[85–89] Ag nanowires,[90] Ag nanoclusters,[91] gold (Au) nanorods,[92] molybdenum disulfide (MoS_2) nanosheets,[93–95] copper sulfide (CuS) nanoparticles,[96] zinc oxide (ZnO) nanomaterials,[97–99] CeO_2 nanoparticles,[100] and metal–organic frameworks (MOFs).[101–103] Moreover, silicon-based nanomaterials include silica nanoparticles,[104,105] polyhedral oligomeric silsesquioxane (POSS),[106] bioactive glass nanoparticles (BGNs)[107] and nanoclay.[108]

Representative preparation methods of nanocomposite hydrogels were divided into three categories: (1) nanomaterials were not grafted with chemical functional groups and then dispersed in hydrogel precursor solution, followed by physical crosslinking to form nanocomposite hydrogels. For example, Haraguchi *et al.* first used nanoclay as a physical crosslinker to fabricate nanocomposite hydrogels with superior mechanical performance in 2002, which was a significant study for nanocomposite hydrogels;[109] (2) nanomaterials are embedded in the hydrogel matrix through physical interactions including hydrogen bonding, hydrophobic interactions, and electrostatic interactions;[110–112] (3) nanomaterials are first functionalized and loaded into the hydrogel matrix through chemical interactions, including imine bonds (Schiff-base interaction), disulfide bonds, and borate–catechol.[32] The physical interaction and chemical interaction between natural polymers and nanomaterials are shown in Fig. 4.

Numerous achievements of NNPHs for skin wound healing have been made by scientists and researchers in recent years. This review highlights and focuses recent publications related to skin wound healing of NNPHs. Initially, the functions and requirements of NNPHs as wound dressings are introduced and discussed. Second, NNPHs are classified based on the types of nanomaterials. Finally, the potential issues of NNPHs are concluded, and future research is proposed to prepare idealized multifunctional NNPH wound dressings.

2. Functions and requirements of NNPHs as wound dressings for skin wound healing

In this section, the functions and requirements of NNPHs as wound dressings are introduced and discussed in detail, including biocompatibility, hemostatic and adhesive performance, antibacterial properties, anti-inflammatory and antioxidant properties, moisturizing ability and air permeability, stimuli-responsive properties, electrical conductivity, and self-healing, as shown in Fig. 5.

2.1 Biocompatibility

As biomaterials, the basic requirement of NNPHs should be biocompatibility so that they would not cause adverse effects on the human body.[113] The composition, structure, surface properties, stability, and mechanical properties can affect the biocompatibility of NNPHs.[114–116] NNPHs serve as wound dressings that come into contact with healthy human skin, damaged tissue and blood, and they might cause inflammation, hyperplasia, thrombosis, and calcification in surrounding tissues and blood.[117] Therefore, it is significant to evaluate the biocompatibility including histocompatibility, cytocompatibility and hemocompatibility of NNPHs before clinical trials. The good histocompatibility of NNPHs ensures that they will not cause severe toxicity, inflammation, or immune response during use.[118] The good cytocompatibility of NNPHs means that they can maintain cell communication, viability, proliferation, and differentiation.[119,120] Blood plays an important role in the transport of nutrients, oxygen, and waste, so it is necessary to maintain the stability of the blood environment.[121,122] The good blood compatibility of NNPHs requires that NNPHs will not cause damage to blood, such as changing the composition of blood and destabilization of the blood environment, leading to blood coagulation.[123,124] It is worth noting that the composition of blood is very complex, including blood cells, genetic components, proteins, electrolytes, enzymes, and nutrients, so NNPHs should also undergo strict *in vivo* blood compatibility evaluation before clinical use.[125,126]

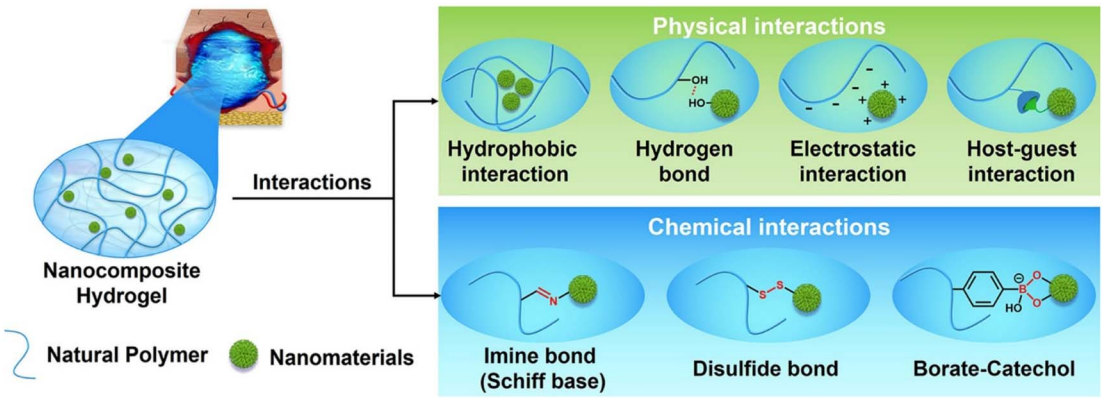

Fig. 4 Illustration of representative interactions between natural polymers and nanomaterials.

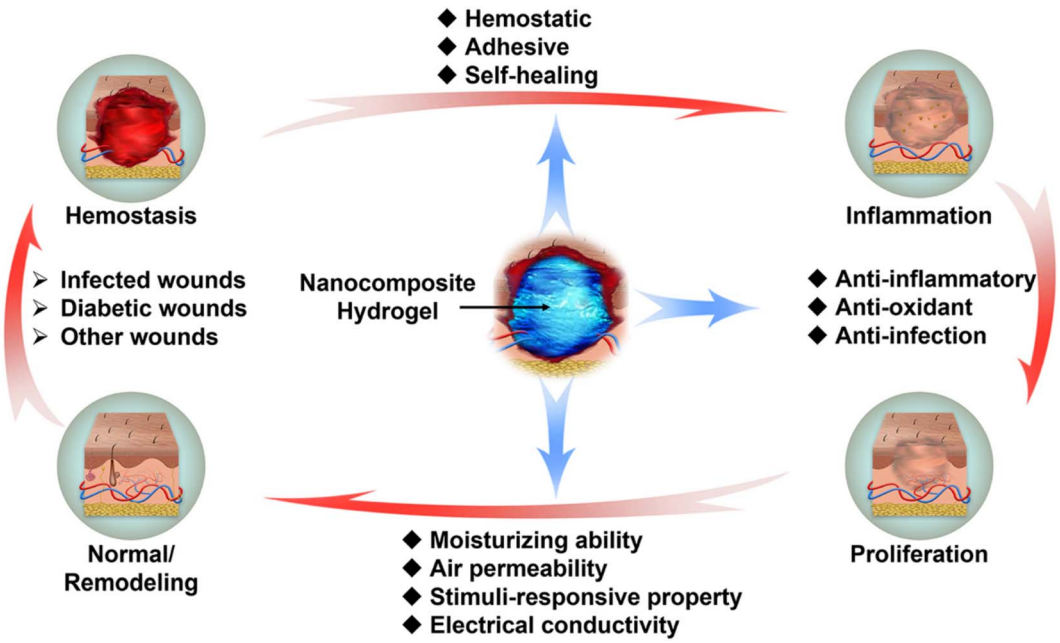

Fig. 5 Illustration of functions and requirements of NNPHs as wound dressings for four consecutive stages of wound healing.

2.2 Hemostatic and adhesive performance

Hemostasis is the first stage of wound healing. Specifically, hemostasis controls bleeding at the injury site, closing ruptured blood vessels through the formation of blood clots, thereby preventing bleeding.[127–129] When injury occurs, platelets in the blood aggregate and become activated at the bleeding site, and subsequently participate in all stages of hemostasis including: (1) activated platelets secreting chemicals that induce vasoconstriction, thereby reducing blood loss; (2) activated platelets forming adhesions with each other and clumping together to form hemostatic platelet plugs and attracting other nearby platelets through secreted substances to accelerate the formation and spread of hemostasis by forming a positive feedback loop; (3) the surface of activated platelets acting as coagulation sites to form blood clots and stop bleeding.[5,121,130]

NNPH dressings with hemostatic effects have positive effect on wound healing. Studies have shown that hemostatic properties of NNPHs can be achieved not only by physical sealing, but also by enriching coagulation factors through the absorption of wound exudates.[49] Notably, adhesive NNPHs can be attached to the wound site seamlessly, which can avoid the potential infection risk caused by the external environment. Moreover, they can also seal the wound quickly to achieve hemostasis.[131,132] Moreover, in the past 10 years, inspired by the excellent dry and wet adhesive properties of mussels, biomimetic NNPHs were designed and fabricated to mimic the 3,4-dihydroxyphenyl chemical structure of mussel foot proteins, which was considered to be the origin of strong adhesiveness due to strong interfacial interactions with skin tissues through hydrogen bonding, cation–π interactions, and Schiff-base bonding.[133] In addition to mussel inspired chemistry, Schiff-base interactions between the aldehyde groups of NNPHs and $-NH_2$ groups of native skin tissues are believed to be another adhesive mechanism.[5]

2.3 Antibacterial properties

Although bacteria are a normal part of the skin and wound, it has been suggested that a value of 10^5 bacteria should be considered as a critical point between normal and clinical infections.[3,134,135] Bacteria can cause persistent inflammation at the site of infection after wound infection, delaying the wound healing process, and severe inflammation can even result in non-healing wounds and serious complications.[136,137] Physical or chemical methods have been applied to kill or hinder the growth of bacteria, and reduce their activity.[137,138] Owing to the abuse of antibiotics, drug-resistant bacteria induced wound infection is a great challenge for wound healing.[139] Although clinical antibacterial drugs can control infection effectively, the drug resistance of bacteria is becoming an increasing problem.[135] Thence, it is of great significance to propose better antibacterial strategies. Integration of bioactive antibacterial components in NNPHs has been utilized to address drug resistance of bacteria and accelerate wound healing.[17,48] Representative bioactive antibacterial materials include metal-based nanomaterials (Ag, Zn, Au, and Cu, *etc.*),[140,141] photothermal antibacterial agents (PDA, CNTs, and GO, *etc.*),[142,143] photodynamic antibacterial agents (MoS_2 and TiO_2, *etc.*),[144,145] antibacterial polymers (chitosan, polyethyleneimine (PEI) and ε-polylysine (EPL), *etc.*),[146–149] and extracts from natural products (honey and essential oil, *etc.*).[150,151]

2.4 Anti-inflammatory and antioxidant performances

The second stage of wound healing is inflammation.[152] Inflammatory cells would kill bacteria or other harmful agents,

followed by healing injured wounds.[153] Inflammation causes redness, pain, warmth, and swelling, and can lead to an increase and accumulation of reactive oxygen species (ROS), which cause damage to skin tissue.[154] However, low levels of ROS are believed to have a positive effect on wound healing.[155] Antioxidant agents can consume accumulated ROS and restrain the production of ROS, reducing inflammation to protect cells and promote wound repair.[156] The representative natural antioxidants are mercaptan compounds, vitamins, and enzymes.[157]

2.5 Moisturizing and air permeability

Gauze is often used as a wound dressing to simply cover the wound for traditional wound healing in a dry environment.[158] Because gauze cannot prevent the evaporation of water, the wound surface would be dehydrated easily, causing large numbers of cell death and scab of wound, which cannot provide an ideal environment for wound healing.[159] In addition, gauze cannot effectively prevent bacterial infection, and it can cause pain when changing gauze due to its adherence to granulation tissue, which even causes multiple injuries and hinders the wound healing process.[160–162]

Since scientists first discovered that wounds show a faster healing rate in a wet environment than in a dry environment in 1962, many scientific studies and clinical trials have been carried out to verify the wound healing mechanism in a wet environment.[163] Research has shown that wound healing in a wet environment can mimic and maintain the physiological state of wounds, which can prevent wounds from drying up, avoid scab formation and scarring, and reduce tissue necrosis.[164] In addition, it is beneficial to maintain the enzyme activity in wound exudate, clear necrotic tissue, stimulate growth factor activity, promote angiogenesis, and fibroblast and epithelial cell growth, accelerate epithelialization and collagen generation, reduce bacterial infection, maintain wound temperature, and reduce pain, and finally accelerate wound healing.[165] NNPHs are one of the wet wound dressings, which could maintain a moist healing environment and absorb exudate for wound healing.

Apart from their moisturizing ability, the air permeability of NNPHs is also important for skin tissue regeneration because healthy skin possesses respiratory functions that can absorb oxygen and release carbon dioxide.[166] While oxygen plays an important role in skin repair and regeneration processes, oxygen can interact with a variety of cytokines, promote cell proliferation, participate in the synthesis of collagen, and accelerate angiogenesis and epithelialization.[167] Oxygen supply affects the rate of wound healing. Researchers have reported that oxygen-permeable dressings can significantly promote wound healing compared to oxygen-impermeable dressings.[168] NNPHs were engineered to create a moist environment with gas exchange performance mimicking the physiological environment of wounds.

2.6 Stimuli-responsive properties

Stimuli-responsive properties of NNPHs, which can respond to environmental stimuli such as temperature, light, and pH are also an interesting function for wound healing.[35,169–171] This section mainly highlights the heat, light, and pH responsiveness of NNPHs because of their interesting performance in smart wound dressings.

Some polymer solutions can undergo a phase transition from sol to gel at the physiological temperature of 37 °C, and they can be injected into wound and form hydrogels immediately, which greatly simplifies the application of wound dressings and makes treatment simple and convenient.[83] On the other hand, some thermoresponsive hydrogels exhibit shrinking behavior at body temperature, causing pre-shrink stress of skin tissue to promote wound closure and healing.[172] The typical thermoresponsive polymers include agar, gelatin, poly(*N*-isopropylacrylamide) and F127.[173]

A variety of nanomaterials (MXenes, Au nanomaterials, MWCNTs, rGO, and PDA nanomaterials) can demonstrate photothermal properties, which can convert light to heat.[174–176] Taking advantage of this phenomenon, NNPHs could enhance their antibacterial performance by scavenging bacteria at high temperature for photothermal therapy.[175–177] In order to avoid damage to the skin due to photothermal therapy at high temperature, photodynamic therapy was also proposed, where photosensitizers such as TiO_2 and ZnO nanomaterials could transform photons to ROS and free radicals for photodynamic therapy at normal temperature.[4] It should be noted that the ROS level for photodynamic therapy should be on-demand controlled, because overloaded ROS might have a negative impact on wound healing.[4]

The pH responsiveness of NNPHs is also involved in wound healing owing to pH changes during infected and/or diabetic wound tissue healing processes; for example, the pH of healed uninfected wounds is between 5.5 and 6.5, while the pH of unhealed infected wounds is higher than 7.0.[3,178] The typical pH responsive natural polymers of NNPHs are hyaluronic acid, chitosan, and sodium alginate on account of rich $-NH_2$ and/or –COOH groups on their structures.[179] Scientists usually load drugs in pH responsive NNPHs for pH-controlled drug release for wound healing.

2.7 Electrical conductivity

Electrically conductive NNPH dressings are beneficial for wound healing and repair, because skin tissue is electrically conductive, enabling function and communication of skin.[50] In addition, the proliferation and differentiation of cells is associated with the electrically conductive environment.[180,181] As mentioned before, the third stage of wound healing is proliferation, which can be verified by granulation tissue formation, where newly granulation tissue will replace damaged tissue.[3] Lots of nanomaterials such as MXenes, nanoscale metallic materials, nanoclay, CNTs, and rGO are electrically conductive, and adequate studies have shown that electrically conductive nanomaterials can optimize the electrical conductivity of NNPHs.[50]

2.8 Self-healing properties

Another requirement of NNPHs is to have good self-healing ability to avoid structural and functional failure under

external tension and pressure at the wound.[182] NNPHs with self-healing properties were carefully designed and fabricated to achieve structural integrity.[183] NNPHs can heal the network structure by themselves to maintain their functions and protect wounds from the outside invasion of harmful components.[184] To date, the self-healing chemistry of NNPHs has focused on physical interactions and/or chemical interactions; for instance, hydrogen bonding, electrostatic interactions, π–π interactions, host–guest interactions and hydrophobic interactions are representative physical interactions, while Schiff-base bonds, S–S bonds and borate bonds are typical chemical interactions.[185]

All in all, specific functions and requirements for NNPHs were summarized. Although it is a challenge to integrate all the functions in one system of NNPH, researchers have been dedicated to preparing multifunctional NNPH platforms for idealized wound dressings in the past 10 years.

3. Preparation and performance of NNPHs according to their nanomaterials

In this section, the design, preparation and capacities of representative NNPHs based on different nanomaterials for skin wound healing and repair are highlighted. The categories of NNPHs are classified as carbon-based, metal-based, MXene-based and silicon-based, as demonstrated in Tables 3–6 according to recent studies.

3.1 Carbon-based NNPHs for wound healing

Due to the decent biocompatibility, and photothermal and electrical conductivity of CNTs, GO and rGO, they have been widely applied in NNPHs for wound healing.[3] Representative research on carbon-based NNPHs for wound healing is summarized in Table 3. CNTs, tubes composed of carbon with a nanometer diameter, high electrical conductivity, astonishing tensile strength and modulus, and desirable thermal conductivity, have attracted much interest in the biomedical field, including wound healing.[186–188] However, the hydrophobic and insoluble limitations of CNTs lead to poor dispersion in various solvents.[81] Therefore, NNPHs with homogeneous performance were fabricated by chemical modification with hydrophilic groups such as –OH, –COOH, and $–NH_2$ or using surfactants such as F127 to increase the dispersion of CNTs.[57,80] For example, He *et al.* prepared an NNPH network through a Schiff-base reaction using aldehyde F127-dispersed CNTs and *N*-carboxyethyl chitosan for infected full-thickness wound healing (Fig. 6A and B). The NNPH exhibited the highest electrical conductivity of 8.45×10^{-3} S m^{-1}, the largest adhesive strength of 8.5 kPa, photothermal antibacterial properties with 100% of killing ratio of bacteria in just 10 minutes and pH-responsive drug release behavior to kill bacteria, and the lowest blood loss of 143.9 ± 60.9 mg, 140 ± 39.7 mg, and 207 ± 19.3 mg for the mouse liver trauma model, mouse tail cutout model, and mouse liver incision model, respectively. Besides, the multifunctional NNPH was further applied in bacterial infected skin wound healing, where bacteria can cause persistent inflammation at the infected site and postpone wound healing. The macroscopic wound contraction of NNPHs was 100% after 14 days of healing. Microscopic wound healing results were also presented, and the thicknesses of granulation tissue and epithelium were 778 μm and 110 μm after 7 days of healing, respectively. After 14 days of healing, the dermis was formed, and blood vessels, hair follicles, *etc.*, in the NNPH group were similar to those of normal healthy skin.[57] In addition, Liang *et al.* optimized the dispersity and bioactivity of CNTs by coating with PDA, and further prepared the NNPH using dopamine functionalized gelatin, chitosan and PDA coated CNTs through self-polymerization. The NNPH displayed antioxidant properties by scavenging 86.5% and 100% of free radicals when the concentration of NNPH was 3 mg mL^{-1} and 5 mg mL^{-1},

Table 3 Composition of NNPHs based on carbon-based nanomaterials for wound healing[a]

Nanomaterials	Polymers and/or monomers	Wound healing model	Healing period	Ref.
rGO@PDA	HA–DA	Full-thickness skin defect wound	14 days	12
PF127/CNTs	QCSG and PF127	Full-thickness skin defect wound	15 days	49
PF127/CNTs	CEC and PF127	*S. aureus* infected wound	14 days	57
GelMA/CNTs	GelMA and AM	*S. aureus* infected wound	12 days	58
GO–CD	QCS–CD and QCS–AD	Full-thickness skin defect wound	14 days	60
CQD	CMCS and ODex	*S. aureus* infected wound	14 days	61
GO–β-CD–BNN6	GelMA and HA–DA	*S. aureus* infected wound	14 days	62
PDA@CNTs	GT–DA and CS	*S. aureus* infected wound	14 days	80
GO	QCSG and GelMA	MRSA infected wound	14 days	82
rGO@PDA	F127–EPL	Diabetic wound	21 days	83
rGO@PDA	QCS and *N*IPAM	Full-thickness skin defect wound	14 days	172
rGO@PDA	CS–DHCA–LAG and PEGS–PBA–BA	Diabetic foot wound	21 days	178

[a] rGO: reduced graphene oxide, PDA: polydopamine, HA: hyaluronic acid, DA: dopamine, PF127: poly(ethylene oxide)–poly(propylene oxide)–poly(ethylene oxide), CNTs: carbon nanotubes, QCSG: glycidyl methacrylate functionalized quaternized chitosan, CEC: *N*-carboxyethyl chitosan, GelMA: gelatin methacryloyl, AM: acrylamide, GO: graphene oxide, CD: β-cyclodextrin, QCS: quaternized chitosan, AD: amantadine, CQD: carbon quantum dots, CMCS: carboxymethyl chitosan, ODex: oxidized dextran, BNN6: *N*,*N*′-di-*sec*-butyl-*N*,*N*′-dinitroso-1,4-phenylenediamine, GT: gelatin, CS: chitosan, EPL: ε-polylysine, *N*IPAM: *N*-isopropylacrylamide, CS–DHCA–LAG: chitosan–dihydrocaffeic acid–L-arginine, PEG: polyethylene glycol, PEGS–PBA–BA: PEG2000–sebacic acid–glycerol–phenylboronic acid–benzaldehyde.

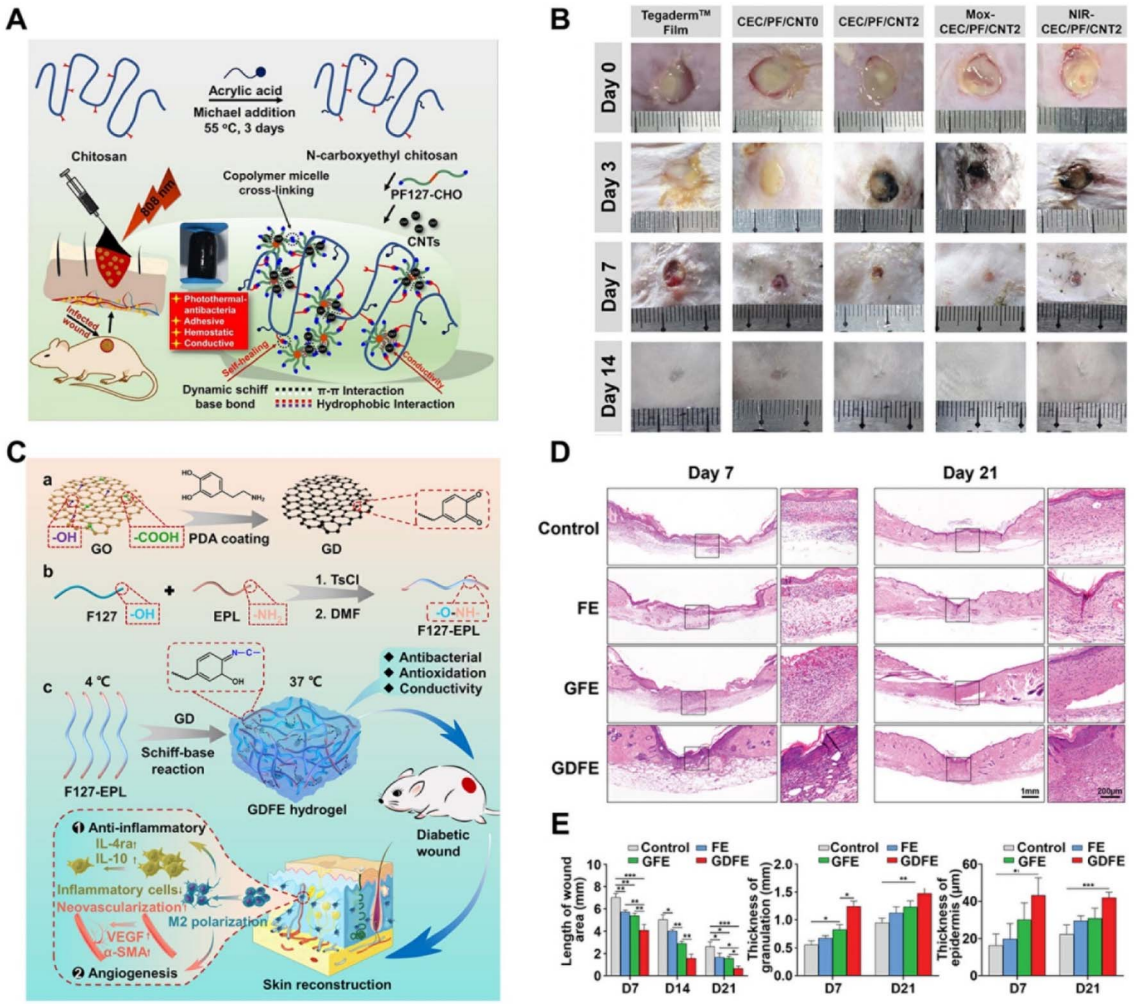

Fig. 6 Carbon-based NNPHs for wound healing. (A) Synthesis schematic of a CNT-based NNPH for wound healing; (B) the photograph of wound closure on the 0th, 3rd, 7th and 14th days;[57] Copyright 2020, Elsevier. (C) Synthesis schematic of a GO-based NNPH for diabetic wound healing; (D) hematoxylin–eosin staining of wound on the 7th and 21st days; (E) quantification of length, granulation and epidermis thickness of wounds.[83] Copyright 2021, John Wiley and Sons.

respectively. Moreover, NNPHs also showed electrical conductivity from 0.062 to 0.072 S m^{-1}, adhesive strength from 3.9 kPa to 6.5 kPa, the lightest blood loss of 170 mg in the liver blood-letting model, and photothermal antibacterial properties with a killing ratio of nearly 100% in just 5 minutes. Furthermore, the infected skin wound healing study was also performed, where a significant wound closure and granulation tissue thickness could be observed in the NNPH group after 7 and 14 days of healing. Histomorphological observation was further performed to evaluate wound healing, and the NNPH group demonstrated obvious dermis and epidermis tissue regeneration.[80]

Another fascinating carbon-based nanomaterial is graphene, research on which was awarded the Nobel Prize in 2010; graphene is made of carbon atoms with a two-dimensional hexagonal lattice structure.[189] Due to its high electrical conductivity, mechanical strength, and thermal conductivity, graphene is an ideal candidate for application in composite materials, biomedical engineering, electronic industry, and so forth.[190] However, graphene suffers from limitations such as poor water solubility, non-biodegradability, potential long-term toxicity, and inefficient preparation processes.[189] To overcome these challenges, researchers fabricated GO and rGO to ameliorate the dispersity of graphene related nanomaterials in water and solvents.[82,119] For instance, Liang *et al.* prepared an injectable NNPH through free radical polymerization using well-dispersed GO, methacrylate gelatin and methacrylate quaternized chitosan to promote the MRSA-infected mouse full-thickness wound healing. The NNPH had electrical conductivity from 0.0097 to 0.1007 S m^{-1}, inherent antibacterial properties against normal bacteria with a 95% killing ratio and drug resistant bacteria with a >90% killing ratio, and photothermal antibacterial properties against all types of bacteria with a 100% killing ratio after exposure to NIR light for 10 minutes. A skin wound healing model for drug-resistant bacterial infection was studied, in which wound closure and collagen content in the NNPH group were significantly better than those in the control group. Besides, obvious hair follicles and blood vessels could be

observed after 14 days in the NNPH group, indicating the repair of skin tissue.[82] GO with hydrophilic functional groups increased its dispersity but sacrificed its electrical conductivity; thus, reduced GO (rGO) was fabricated to optimize its electrical conductivity without affecting its dispersity.[3] Coating PDA on GO is a typical method to prepare rGO with antioxidant performance and excellent dispersity in water.[83,172] For example, Li *et al.* prepared an NNPH using PDA coated GO, quaternized chitosan, and *N*-isopropylacrylamide. The NNPH exhibited self-healing performance within 2 hours through Schiff-base dynamic chemical interactions, hydrogen bonding and cation–π physical interactions, antioxidant performance with 98% free radicals consumed with only 5 mg mL^{-1} of NNPH, electrical conductivity of 5.0–5.6 mS cm^{-1}, innate antibacterial performance with a killing ratio more than 85% for *Staphylococcus aureus* (*S. aureus*) and *Escherichia coli* (*E. coli*), NIR light induced antibacterial performance with entirely killing of bacteria within 10 minutes, decent *in vitro* hemocompatibility with a small hemolysis ratio of ~1.6, good air permeability compared to Tegaderm™ film, and an adhesive strength of 9.68 kPa. Interestingly, the NNPH was built for temperature induced wound closure at 37 °C because of the self-shrinking behavior of P*N*IPAM with 51% of the wound area contracted on the second day, while the control group had only 20% of the contracted wound area. In addition, an acute full-thickness skin defect model was further studied for wound healing. Conventional acute wound models are usually similar to surgery or trauma wounds, where wounds occur and heal in just a few days or weeks. In addition, the NNPH group showed complete wound closure on day 14, while wounds in the control group were still not 100% closured.[172]

In addition to acute wound healing and chronic infected wound healing, a NNPH with PDA coated rGO was also synthesized for chronic diabetic wound healing, in which wounds would take a longer time to repair for diabetic patients.[83,178] Microvascular dysfunction caused by hyperglycemia in diabetic patients can lead to wound ischemia and delayed healing, which has become a serious threat to the health of patients.[149] Therefore, it is important to propose advanced strategies to accelerate diabetic wound healing.[83] Among diabetic wounds, diabetic foot wounds commonly occur in diabetic patients, usually at the bottom of the foot.[178] For example, Liang *et al.* prepared an NNPH using dihydrocaffeic acid and L-arginine grafted chitosan, benzaldehyde groups and phenylboronic acid functionalized sebate and PDA coated rGO through the double dynamic bonds of Schiff base and phenylboronate ester for athletic diabetic foot wound healing. The NNPH demonstrated desirable biocompatibility and biodegradability (<30% of remaining weight after 15 days of degradation), water absorption (a swelling ratio of 1081%), self-healing properties, on-demand removal ability (NNPH can be removed using solutions containing acid and/or glucose), pH and glucose dual responsive characteristics (highest metformin release at a pH of 5.5 and better metformin release within glucose), electrical conductivity (~10^{-1} S m^{-1}), antibacterial properties (killing ratio of >99% with drug resistant bacteria), adhesive and hemostatic ability (an adhesive strength of 17.51 kPa), and anti-oxidation properties (>90% of free radicals eradicated with a NNPH concentration of 2 mg mL^{-1}, and nearly complete free radicals consumed when NNPH concentration is 4 mg mL^{-1}). In addition, the synthesized NNPH exhibited an obvious positive effect on diabetic foot wound healing, where 98% of the wound was closured after 3 weeks of healing. In addition, the thickest granulation tissue, best angiogenesis results, and highest number of follicles could be found in the NNPH group.[178] Apart from diabetic foot wound healing, Tu *et al.* prepared an injectable and self-healing NNPH at 37 °C using EPL grafted F127 and PDA coated GO through a Schiff base reaction for diabetic wound healing (Fig. 6C and E). The NNPH possessed antioxidant properties with an antioxidant rate of 92%, broad-spectrum antibacterial capacity with a 99% killing ratio for *E. coli*, *S. aureus*, and methicillin-resistant *Staphylococcus aureus* (MRSA), electrical conductivity of 0.04 S m^{-1}, and promoting M2 polarization of macrophages and proliferation, migration, and angiogenesis of endothelial cells. In addition, the NNPH can promote the full-thickness diabetic wound repair with a fastest period of 17.5 days for completed wound closure.[83]

3.2 Metal-based NNPHs for wound healing

Ag, Au, ZnO, TiO_2, MoS_2, CuS, and ZnS based nanomaterials are representative materials for synthesizing NNPHs for wound healing because of their biocompatibility, electrical conductivity, photothermal and/or photodynamic properties and antibacterial performance.[3,93,95,191] The typical studies of metal-based NNPHs for wound healing are shown in Table 4.

Ag-based nanomaterials have been used in biomedical applications for many years due to their antibacterial, anticancer, and accelerated wound healing performances.[191] Qi *et al.* fabricated an NNPH using Ag-decorated polydopamine nanoparticles and cationic guar gum to combat bacterial infection and promote wound healing. The addition of Ag can effectively improve the photothermal conversion efficiency of PDA nanoparticles. The NNPH displayed self-healing and injectable properties, excellent photothermal-assisted antibacterial properties with >99% of *E. coli* and *S. aureus* being eliminated after exposure to NIR light for 3 minutes, good hemocompatibility and cytocompatibility with a hemolysis ratio less than 5% and ~100% cell viability, respectively. Furthermore, the bacteria-infected skin wound model was used to study the wound healing efficiency of the NNPH. The NNPH with the assistance of NIR light (NNPH + NIR) possessed superior bactericidal activity and a rapid wound healing rate with wound closure after 12 days. Besides, the wounds treated with NNPH + NIR also showed the most collagen deposition and the highest CD31 expression but the lowest IL-6 expression, indicating that the NNPH + NIR can accelerate the healing of infected wounds.[191] In addition, other precious metal Au-based nanomaterials were also developed for skin wound healing because of their chemical stability, biocompatibility and photothermal properties.[68]

MoS_2, ZnS, CuS, ZnO, and TiO_2 based nanomaterials are typical metal oxides and metal sulfides that have been prepared

Table 4 Composition of NNPHs based on metal-based nanomaterials for wound healing[a]

Nanomaterials	Polymers and/or monomers	Wound healing model	Healing period	Ref.
Ag/Ag@AgCl/ZnO	CMC	Full-thickness skin defect wound	14 days	67
Au–Pt NPs	CMCS and OHA	Diabetic wound	15 days	68
MoS_2 NCs	SA	Diabetic wound	14 days	69
Eu_2O_3 NRs	HA–AL and PF127	Full-thickness skin defect wound	14 days	70
Ag NPs	Agar and FA	Full-thickness skin defect wound	16 days	85
Ag NPs	GT–DA and GG	*S. aureus* infected wound	10 days	87
Ag nanowires	MA-ALG	*E. coli* and *S. aureus* infected wound	2 days	90
Ag NCs and MF@Lip	CS and PEG	*S. aureus* infected wound	8 days	91
MoS_2@Au@BSA	ODex and glycol chitosan	Diabetic wound	8 days	93
MoS_2@TA/Fe	ODex and PVA	*S. aureus* infected wound	8 days	95
CuS NPs	ODex and PEG with amino end groups	Full-thickness skin defect wound	14 days	96
ZnO QDs@GO	CS	*S. aureus* infected wound	14 days	97
Tetrapodal ZnO	GelMA	Full-thickness skin defect wound	14 days	98
ZnO NPs	SA and CSO	Deep second-degree scald wound	19 days	99
Au@ZIF-8	OSA and GelMA-CDH	*S. aureus* infected wound	14 days	102
Au NCs@PCN	PVA and ALG	Diabetic wound	21 days	103
PDA@Ag	CG	*S. aureus* infected wound	12 days	191

[a] CMC: carboxymethyl cellulose, NPs: nanoparticles, CMCS: carboxymethyl chitosan, OHA: oxidized hyaluronic acid, NCs: nanoclusters, SA: sodium alginate, NRs: nanorods, HA–AL: hyaluronic acid–alendronate sodium, PF127: poly(ethylene oxide)–poly(propylene oxide)–poly(ethylene oxide), FA: fumaric acid, GT–DA: gelatin–dopamine, GG: guar gum, MA-ALG: methacrylated alginate, MF: mangiferin, Lip: liposome, CS: chitosan, PEG: polyethylene glycol, BSA: bovine serum albumin, ODex: oxidized dextran, TA: tannic acid, PVA: poly(vinyl alcohol), QDs: quantum dots, GelMA: gelatin methacryloyl, CSO: chitosan oligosaccharide, ZIF: zeolitic imidazolate framework, OSA: oxidized sodium alginate, GelMA-CDH: gelatin methacryloyl-carbohydrazide, PCN: zirconium-based porphyrin metal–organic frameworks, CG: cationic guar gum.

to develop NNPH platforms for wound healing on account of their photodynamic properties and/or photothermal properties, antibacterial properties, and promoting ability.[63,95–99] Li *et al.* constructed a multifunctional NNPH platform based on tannic acid-chelated Fe-decorated MoS_2 nanosheets with dual enzyme activities and a multifunctional hydrogel including polyvinyl alcohol (PVA), dextran (Dex) and borax for bacteria-infected wound healing. The MoS_2@TA/Fe nanosheet had a peroxidase-like ability to catalyze H_2O_2 to ·OH under an acid environment and catalase-like ability to catalyze H_2O_2 to O_2 under a neutral environment. The NNPH showed excellent antibacterial properties with a 100% killing ratio through the combined effect of ·OH, loss of glutathione, and photothermal therapy. The NNPH also showed self-healing properties and shape adaptability due to dynamic boron ester bonds and hydrogen bonds, adhesive properties because of abundant phenolic hydroxyl groups, good blood compatibility and cell compatibility with low hemolytic ratio and high cell viability *in vitro*, anti-inflammatory performance with high expression of IL-10 and low expression of TNF-α *in vitro*, antioxidant performance with scavenging of >80% reactive oxygen species (ROS) and reactive nitrogen species (RNS) with 15 mg mL^{-1} of MoS_2@TA/Fe nanosheets. Finally, *S. aureus*-infected wounds were created to investigate the ability of the NNPH to promote wound healing. With the assistance of H_2O_2 and NIR light, there were negligible bacteria in the NNPH group, which exhibited an excellent ability to prevent infection *in vivo*. In addition, the NNPH demonstrated the best wound healing after 8 days, displaying the smallest wound area, mature epidermal layer formation, more well-defined collagen fibers, highest expression of VEGF and IL-10, and lowest expression of TNF-α *in vivo*.[95]

Furthermore, Li *et al.* further designed an injectable NNPH using defect-rich MoS_2 nanosheets (MoS_2@Au@BSA) loaded with bovine serum albumin (BSA) modified with Au nanoparticles and a hydrogel prepared using oxidized dextran and glycol chitosan for diabetic wound healing through an oxygen self-supplying cascade reaction (Fig. 7). The MoS_2@Au@BSA nanosheets had catalytic abilities similar to those of glucose oxidase, which is able to oxidize glucose to H_2O_2 and gluconic acid, along with the peroxidase-like and catalase-like abilities of MoS_2. Compared to the previously mentioned work, this NNPH could eradicate bacteria and promote infected diabetic wound healing in just 8 days without the help of external H_2O_2 and NIR light due to the accumulated glucose in the diabetic wounds being automatically converted to H_2O_2.[93] ZnO based nanomaterials are another well-known nanofillers to develop NNPHs for wound healing due to their biocompatibility, antibacterial properties, and photoactive properties.[98] In addition, Zn elements have vital significance for cell functions, including growth, metabolism, immunity, and so on.[192] For example, Siebert *et al.* prepared a ZnO based 3D printable NNPH using vascular endothelial growth factor (VEGF) modified antibacterial tetrapodal ZnO and methacrylated gelatin (GelMa). The 3D-printed NNPH demonstrated excellent cytocompatibility of endothelial cells due to the sustainable release of VEGF and antibacterial performance against *S. aureus* and *P. aeruginosa* mainly due to the ROS release. The 3D-printed NNPH also promoted angiogenesis with the highest expression of the marker CD31 after 4 weeks because of the combined effect of VEGF and Zn^{2+}. Finally, the 3D-printed NNPH can inhibit inflammation and promote angiogenesis and cell proliferation to accelerate wound healing. After 2 weeks, the 3D-printed

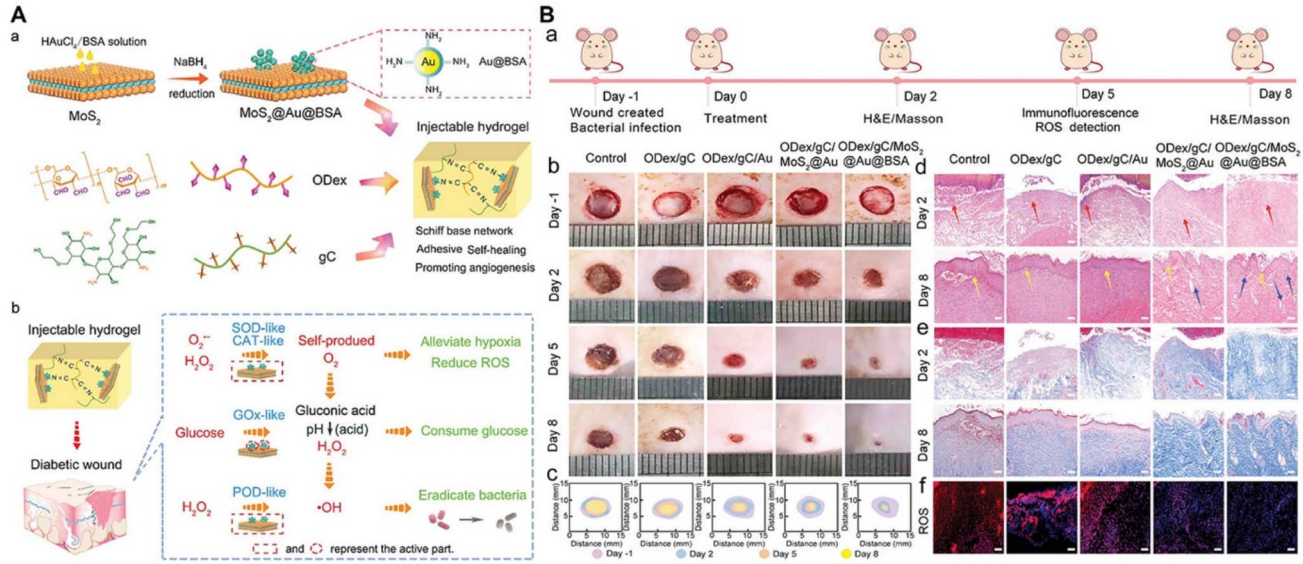

Fig. 7 Metal-based NNPHs for wound healing. (A) Synthesis schematic of a MoS_2-based NNPH for wound healing; (B) the photograph of wound closure and the histologic analyses of wound on the 2nd and 8th days.[93] Copyright 2022, John Wiley and Sons.

NNPH group showed the smallest wound size with only 3.48% of wound area remaining, the thickest epidermis with 101.2 μm of thickness, and the densest dermis with 95.3% per size.[98]

Metal–organic frameworks (MOFs), a class of hybrid materials, consist of central metals and organic struts.[193] MOF-based nanomaterials have ultra-high surface areas, high porosities with uniform pore size, and superior thermal stability.[193] Due to the bactericidal ability of metal ions such as Ag^+, Zn^{2+}, and Cu^{2+}, NNPHs with MOF-based nanomaterials serving as nanofillers have also been studied for wound healing applications.[194–196] Deng *et al.* reported an injectable biomimetic NNPH using metal–organic frameworks (MOFs) with encapsulated Au nanoparticles (Au@ZIF-8) and hydrogels prepared using carbohydrazide-modified GelMa and oxidized sodium alginate through a Schiff-base as well as photo crosslinking. The NNPH displayed photodynamic bactericidal performance, with >99.0% of bacteria eradicated after light exposure (generating ROS) for 20 minutes. Besides, *in vivo S. aureus* infected wound healing studies were conducted to test the wound healing efficiency of NNPHs, where 97.6% of wound area was closured for the NNPH group after 2 weeks.[102]

Taken together, metal-based nanomaterials are good candidates for the manufacturing of multifunctional NNPHs. To achieve integrated functions and performances such as dispersion, photodynamic/photothermal properties, and antibacterial properties, for different types of wound healing, they were elaborately designed and often chemically modified with other functional components. However, there remain potential challenges and limitations for metal-based nanomaterials in wound healing applications due to their potential toxicity.[197]

3.3 MXene-based NNPHs for wound healing

MXenes are a class of 2D inorganic materials consisting of carbides and/or nitrides with transition metals.[198] Compared to the hydrophobicity of previously mentioned nanomaterials, MXenes have desirable hydrophilicity due to the presence of hydrophilic –OH groups on their surface, as well as good biocompatibility, facile functionalization properties, photothermal properties, electrical conductivity and stability.[199] The primary papers of MXene-based NNPHs for wound healing are shown in Table 5.

Table 5 Composition of NNPHs based on MXene-based nanomaterials for wound healing[a]

Nanomaterials	Polymers and/or monomers	Wound healing model	Healing period	Ref.
MXene@CeO_2	OSA and PF127–PEI	MRSA infected wound	14 days	71
MXene@PDA	OHA and PEI–GTA	MRSA infected wound	14 days	73
MXene@PDA	HA–DA	*S. aureus* infected wound	9 days	74
MNPs@MXene and Ag NPs	P*N*IPAM and ALG	Deep diabetic wound	12 days	75
MXenes	rBC	Full-thickness skin defect wound	14 days	84

[a] OSA: oxidized sodium alginate, PF127–PEI: poly(ethylene oxide)–poly(propylene oxide)–poly(ethylene oxide)–polyethyleneimine, PDA: polydopamine, OHA: oxidized hyaluronic acid, GTA: glycerol modified with –C≡C–, HA–DA: hyaluronic acid–dopamine, MNPs: Fe_3O_4@SiO_2 magnetic nanoparticles, NPs: nanoparticles, P*N*IPAM: poly(*N*-isopropylacrylamide), ALG: alginate, rBC: regenerated bacterial cellulose.

In recent years, MXene-based NNPHs have been extensively studied in skin wound repair.[71,73,84] For example, Mao *et al.* developed a biodegradable and electroactive NNPH using regenerated bacterial cellulose and MXenes ($Ti_3C_2T_x$) to accelerate skin wound healing under electrical stimulation. The NNPH displayed compressive-recoverable flexible mechanical capacity, electrical conductivity from 0.00283 S m^{-1} to 0.0704 S m^{-1}, and degradability with a degradation period of 210 minutes. Moreover, the full-thickness wound treated with the NNPH under electrical stimulation was closured 93.8% after 2 weeks, which exhibited the best wound closure.[84] In addition, Zhou *et al.* prepared a conductive antibacterial NNPH using PDA coated MXenes ($Ti_3C_2T_x$), poly(glycerol-ethylenimine) and oxidized hyaluronic acid through a Schiff-base reaction to promote MRSA-infected wound healing. The NNPH exhibited excellent self-healing properties, an electrical conductivity of 2.89 S m^{-1}, competitive bactericidal properties against *E. coli*, *S. aureus*, and MRSA with a killing ratio of ~99.0%. The NNPH also possessed biodegradability with a degradation period of 7 days *in vivo* and good biocompatibility with the best cell proliferation and the highest collagen III, α-actin, and VEGF gene expression. In addition, the NNPH exhibited a wound closure rate of approximately 96% after 14 days for MRSA-infected skin wounds, and the thickest granulation tissue (~120 μm), the best collagen deposition (~70%) and the highest gene expression of α-actin and CD31, indicating that the NNPH can accelerate the MRSA-infected wound healing.[73] Furthermore, Zheng *et al.* prepared an anti-inflammatory, antibacterial and conductive NNPH using CeO_2-loaded MXene, PEI grafted F127 and oxidized sodium alginate for infection-impaired skin multimodal therapy. The NNPH can promote cell proliferation, cell migration and collagen deposition to accelerate multidrug-resistant (MDR) bacterial infected-wound healing.[71] In addition, Li *et al.* developed an injectable NNPH through oxyhemoglobin/H_2O_2 crosslinking using dopamine-grafted hyaluronic acid and PDA coated MXene nanosheets for the mild photothermal-controlled release of oxygen to promote diabetic wound healing (Fig. 8). The oxyhemoglobin served as a catalyst to fabricate a network of NNPH and oxygen vehicles to release O_2 under exposure to NIR light. The NNPH possessed tissue adhesion ability, self-healing performance induced by hydrogen bonding and π–π stacking, photothermal properties with a maximum temperature of 40.0 °C, controlled O_2 release with a maximum O_2 release of 22.7 mg mL^{-1} under exposure to NIR light, ROS and RNS scavenging performances (~90%), and good hemostatic ability. For the infected diabetic wounds, the NNPH exposed to NIR light exhibited a maximum wound closure rate of about 98.8%, a minimum epidermal thickness of 26 μm, and the highest expression of CD31, collagen and M2 macrophages after 9 days.[74]

Tremendous achievements have been made related to MXene-based nanomaterials, but there are some limitations that should be noted. The MAX etching process might bring in highly toxic and dangerous hydrofluoric acid, which can cause permanent harm and even death to lives easily. In addition, the large scale production of MXenes should be further studied. The hydrofluoric acid free etching method is highly anticipated and meaningful, but few hydrofluoric acid free methods have been reported.

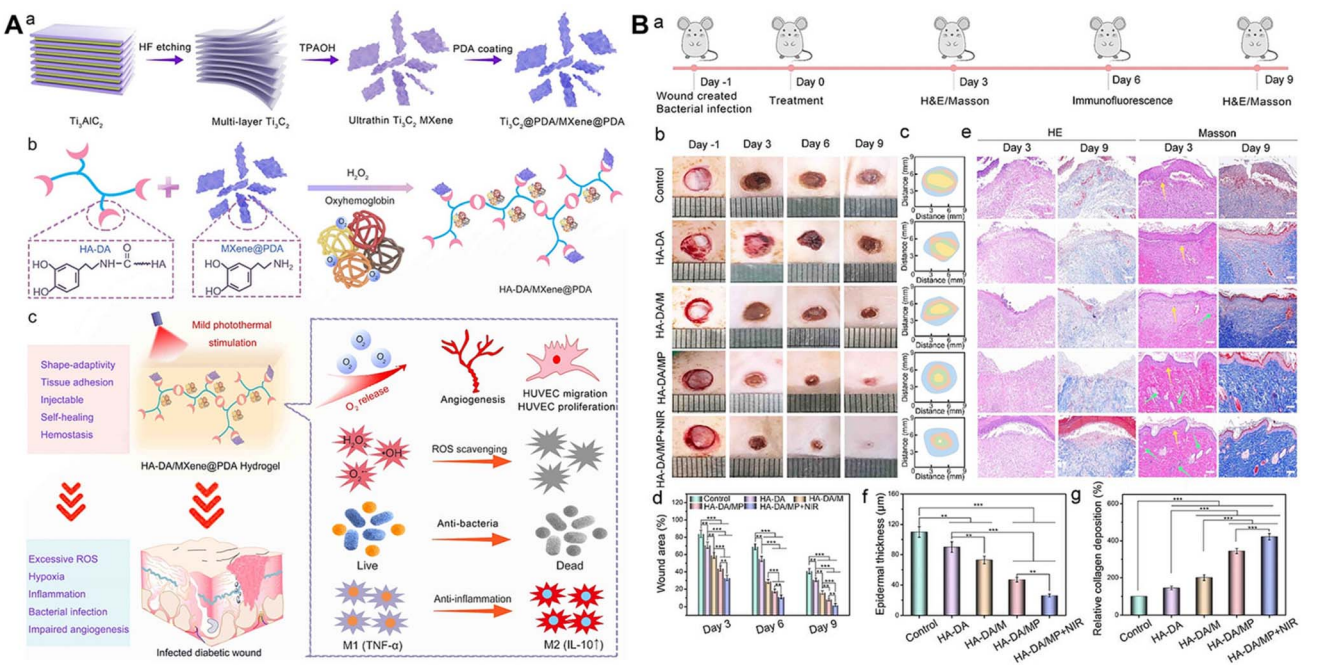

Fig. 8 MXene-based NNPHs for wound healing. (A) Synthesis schematic of an MXene-based NNPH for wound healing; (B) the photograph of wound closure, the histologic analyses, epidermis thickness and collagen deposition of wound on the 3rd and 9th days.[74] Copyright 2022, American Chemical Society.

Table 6 Composition of NNPHs based on silicon-based nanomaterials for wound healing[a]

Nanomaterials	Polymers and/or monomers	Wound healing model	Healing period	Ref.
MCF	HEC, MATMA and PEGDA	Bacteria infected wound	15 days	203
Nanoclay	Col	Diabetic wound	21 days	205
POSS@PDA	TCS and PEGDA	Full-thickness skin defect wound	18 days	207
BGN@PDA	PF127–CHO and PF127–EPL	Full-thickness skin defect wound	14 days	209
BGN–Cu	PEGDA and ALG	Diabetic wound	21 days	210

[a] MCF: mesocellular silica foam, HEC: quaternized hydroxyethyl cellulose, MATMA: 2-(methacryloyloxy)-ethyltrimethylammonium chloride, PEGDA: poly(ethylene glycol)diacrylate, Col: collagen, POSS: polyhedral oligomeric silsesquioxane, PDA: polydopamine, TCS: thiolated chitosan, BGN: bioactive glass nanoparticle, PF127–CHO: poly(ethylene oxide)–poly(propylene oxide)–poly(ethylene oxide) functionalized with –CHO groups, EPL: ε-polylysine, ALG: alginate.

3.4 Silicon-based NNPHs for wound healing

Silicon-based nanomaterials including silica, nanoclay, polyhedral oligomeric silsesquioxane (POSS), and bioactive glass nanoparticles (BGNs) have been widely applied in hemostasis, bone tissue engineering and wound healing due to their cost-effectiveness, biocompatibility, mechanical reinforcement, and stable capacities.[200–202] The main studies of silicon-based NNPHs for wound healing are displayed in Table 6.

Wang *et al.* developed a bioinspired injectable NNPH using quaternized hydroxyethyl cellulose (HEC) and mesocellular silica foam (MCF) for rapid hemostasis without compression and accelerated wound healing. The NNPH possessed excellent swelling and water absorption, excellent bionic hemostatic effects, and good antibacterial properties. In addition, in full-thickness infected wounds, the NNPH can effectively inhibit bacterial infection and the inflammatory response and promote wound healing.[203] Nanoclay is an ultra-fine polar nanomaterial composed of various nanoparticles, which possess diverse mineral components, and good binding ability and dispersibility compared to silica nanoparticles.[204] Ordeghan *et al.* developed an antibacterial NNPH comprised of nanoclay, collagen and tadalafil, which can effectively accelerate the healing time of wounds and promote hair follicle formation and collagen deposition for diabetic wounds under high-intensity interval training.[205] POSS is a biocompatible hybrid nanostructure comprised of silicon and oxygen, which can achieve multifunctionality through covalent chemical modification of the organic groups.[206] Yang *et al.* developed an Ag-loaded NNPH using PEGDA, thiolated chitosan and PDA-modified POSS to accelerate wound healing. The NNPH exhibited excellent mechanical properties, and good adhesive and antibacterial properties, and facilitated cell attachment and proliferation. The NNPH can effectively inhibit the inflammatory response and promote the formation of blood vessels and granulation tissue to promote the full-thickness wound healing.[207]

BGN is a silicate-based inorganic amorphous nanomaterial, which possesses good hemostatic properties and angiogenesis ability, and can promote the expression of bioactive factors related to wound healing.[208] Zhou *et al.* prepared a bioactive polypeptide-based NNPH using PDA coated BGNs, benzaldehyde-modified F127 and EPL-modified F127 through a Schiff-base reaction for the skin-tumor therapy and MRSA-

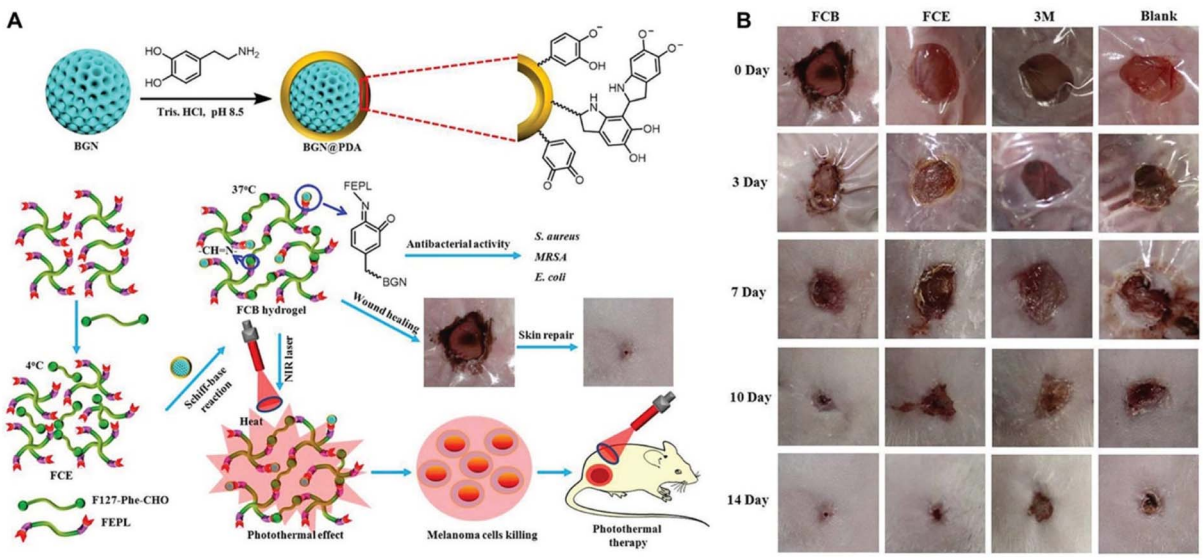

Fig. 9 Silicon-based NNPHs for wound healing. (A) Synthesis schematic of a BGN-based NNPH for wound healing; (B) the photograph of wound closure on the 0th, 3rd, 7th, 10th and 14th days.[209] Copyright 2019, John Wiley and Sons.

infected wound healing (Fig. 9). The NNPH exhibited good injectability and self-healing ability, excellent broad spectrum antibacterial activity, and photothermal performance to inhibit tumor growth. Furthermore, the NNPH exhibited a wound closure rate of approximately 98.8% and regenerated granulation tissue of approximately 240 μm after 14 days for full-thickness skin wounds.[209] Li *et al.* developed an antibacterial NNPH using copper-doped BGN, sodium alginate and polyethylene glycol diacrylate (PEGDA) to promote diabetic wound healing. The NNPH possessed good self-healing performance due to dynamic electrostatic interactions between Ca^{2+}/Cu^{2+} and sodium alginate, excellent antibacterial capacity with an ~100% killing ratio due to the existence of Cu^{2+}, and enhanced endothelial progenitor cell proliferation and angiogenic ability. For full-thickness diabetic wounds, the NNPH can promote the deposition of collagen and the expression of HIF-α/VEGF to restore blood vessel networks, which further accelerated the wound healing.[210] In addition, Chen *et al.* developed hierarchical functionalization of strontium-doped BGN nanohybrids with polypyrrole, PDA and EPL, which exhibited enhanced antioxidant, electrical conductivity, broad-spectrum antibacterial and anti-infective properties. The nanohybrids can not only promote collagen deposition and angiogenesis to accelerate normal wound healing, but also promote MRSA-infected and tumor-impaired wound healing.[211] Niu *et al.* also prepared different element-doped BGNs, including molybdenum-doped or europium and gadolinium-codoped BGN nanoplatforms, which can also efficiently promote MRSA-infected and tumor-impaired skin regeneration.[212] Therefore, NNPHs based on functionalized modified BGN will have important research prospects in various complex skin repair.

Although some of the silicon based materials have been approved by the FDA for clinical use, their nanoscale counterparts with undesirable dispersity should be further considered. Chemical modification with other components, such as PDA, might ameliorate their dispersity and functionality. Similar to other nanomaterials, the system mass production is difficult to implement.

4. Conclusion and outlook

In this review, requirements and functions for wound dressings of NNPHs were first proposed and highlighted, including biocompatibility, hemostatic, tissue adhesive, bactericidal, anti-inflammatory and antioxidant, stimuli-responsive, self-healing, and electrically conductive properties and so forth. Thereafter, NNPHs for wound healing were classified and summarized based on their nanofillers. Although great and ever-increasing NNPHs have been elaborately created to address different types of wounds, NNPHs still have some roadblocks for further investigation. The remaining potential problems are highlighted as follows: (1) cost-effectiveness with high-volume mass production and eco-friendly preparation methods of NNPHs are major challenges, because the production of nanomaterials usually demonstrates complicated time-consuming procedures along with harmful chemicals, moreover, the costs of natural polymers and some chemicals are expensive; (2) stability of performances of NNPHs from batch to batch should be further ameliorated because of the instability of natural polymers, for example, molecular weights of natural polymers are different from batch to batch production; (3) long-term biosafety of NNPHs should be carefully considered because nanomaterials would be accumulated in creatures, which might cause undesirable side effects and toxicity; (4) the exchange and removal of NNPHs might cause secondary damage to wounds because they can adhere to the injury site; (5) wound healing studies for large mammals such as pigs and sheep are rarely reported, and the majority of animal studies are focused on rats skin despite lots of difference between rat skin and human skin. Based on the above-mentioned limitations, the future outlooks of NNPHs for wound healing are proposed: (1) advanced technology and facile eco-friendly methods should be developed to engineer NNPHs with mass production; (2) synthetic polymers are anticipated to be combined with natural polymers to develop NNPHs with better performance for wound healing; (3) further and long-term *in vivo* biocompatibility studies should be put into practice before clinical utilization; (4) design and manufacture of smart wound dressings with detection and monitoring ability for wound conditions without incurring harm during peeled off and exchange is highly expected; (5) it would be better to add large animal skin wound models for wound healing investigation to address the limitations of rat skin.

Although numerous studies and great efforts have been made to engineer NNPHs for wound healing, clinical trials and commercial products still need to be developed. There are some considerations that should be taken into account before clinical translation. First, the therapeutic effect of NNPHs for wound healing should be prioritized. Second, the biosafety, stability and environmental tolerance of NNPHs are anticipated to be further investigated and ameliorated. Last, the cost of products should be reasonable so patients can afford them. At the intersection of materials science and biomedical fields, NNPHs have a promising future with the ever-developing science and technologies. We believe that NNPHs will be in clinical use soon after they are elaborately designed and fabricated for wound healing.

Author contributions

Min Wang: investigation, writing – original draft, visualization. Zexing Deng: investigation, writing – original draft. Yi Guo: investigation, writing – editing. Peng Xu: supervision, conceptualization.

Conflicts of interest

The authors declare no conflict of interest.

Acknowledgements

We acknowledge the financial support of the Natural Science Foundation of Shaanxi Province (grant no. 2022JQ-384), the High-level Talents Foundation for Scientific Research of Xi'an University of Science and Technology (grant no. 2050122015),

the Fundamental Research Funds for the Central Universities (grant no. xzy012021075), and the China Postdoctoral Science Foundation (grant no. 2021M702644).

References

1 Y. Xi, J. Ge, M. Wang, M. Chen, W. Niu, W. Cheng, Y. Xue, C. Lin and B. Lei, *ACS Nano*, 2020, **14**, 2904–2916.
2 Y. Huang, L. Mu, X. Zhao, Y. Han and B. Guo, *ACS Nano*, 2022, **16**, 13022–13036.
3 Y. Liang, J. He and B. Guo, *ACS Nano*, 2021, **15**, 12687–12722.
4 A. Maleki, J. He, S. Bochani, V. Nosrati, M. A. Shahbazi and B. Guo, *ACS Nano*, 2021, **15**, 18895–18930.
5 B. Guo, R. Dong, Y. Liang and M. Li, *Nat. Rev. Chem.*, 2021, **5**, 773–791.
6 P. A. Shiekh, A. Singh and A. Kumar, *Biomaterials*, 2020, **249**, 120020.
7 Y. Yuan, S. Shen and D. Fan, *Biomaterials*, 2021, **276**, 120838.
8 Z. Zhang, J. Xie, J. Xing, C. Li, T. M. Wong, H. Yu, Y. Li, F. Yang, Y. Tian, H. Zhang, W. Li, C. Ning, X. Wang and P. Yu, *Adv. Healthcare Mater.*, 2022, 2201565.
9 Z. Xu, S. Han, Z. Gu and J. Wu, *Adv. Healthcare Mater.*, 2020, **9**, 1901502.
10 X. Zhao, H. Wu, B. Guo, R. Dong, Y. Qiu and P. X. Ma, *Biomaterials*, 2017, **122**, 34–47.
11 J. Qu, X. Zhao, Y. Liang, T. Zhang, P. X. Ma and B. Guo, *Biomaterials*, 2018, **183**, 185–199.
12 Y. Liang, X. Zhao, T. Hu, B. Chen, Z. Yin, P. X. Ma and B. Guo, *Small*, 2019, **15**, 1900046.
13 Y. Xi, J. Ge, Y. Guo, B. Lei and P. X. Ma, *ACS Nano*, 2018, **12**, 10772–10784.
14 J. Qu, X. Zhao, Y. Liang, Y. Xu, P. X. Ma and B. Guo, *Chem. Eng. J.*, 2019, **362**, 548–560.
15 X. Zhao, Y. Liang, Y. Huang, J. He, Y. Han and B. Guo, *Adv. Funct. Mater.*, 2020, **30**, 1910748.
16 Y. Liang, Z. Li, Y. Huang, R. Yu and B. Guo, *ACS Nano*, 2021, **15**, 7078–7093.
17 S. Du, N. Zhou, G. Xie, Y. Chen, H. Suo, J. Xu, J. Tao, L. Zhang and J. Zhu, *Nano Energy*, 2021, **85**, 106004.
18 F. Bao, G. Pei, Z. Wu, H. Zhuang, Z. Zhang, Z. Huan, C. Wu and J. Chang, *Adv. Funct. Mater.*, 2020, **30**, 2005422.
19 R. Yu, Y. Yang, J. He, M. Li and B. Guo, *Chem. Eng. J.*, 2021, **417**, 128278.
20 Y. Yang, Y. Liang, J. Chen, X. Duan and B. Guo, *Bioact. Mater.*, 2022, **8**, 341–354.
21 M. Li, Y. Liang, Y. Liang, G. Pan and B. Guo, *Chem. Eng. J.*, 2022, **427**, 132039.
22 Q. Zeng, X. Qi, G. Shi, M. Zhang and H. Haick, *ACS Nano*, 2022, **16**, 1708–1733.
23 A. Kushwaha, L. Goswami and B. S. Kim, *Nanomaterials*, 2022, **12**, 618.
24 L. Lei, X. Wang, Y. Zhu, W. Su, Q. Lv and D. Li, *Mater. Des.*, 2022, **215**, 110478.
25 L. Lei, Y. Zhu, X. Qin, S. Chai, G. Liu, W. Su, Q. Lv and D. Li, *Chem. Eng. J.*, 2021, **425**, 130671.
26 M. Li, J. Chen, M. Shi, H. Zhang, P. X. Ma and B. Guo, *Chem. Eng. J.*, 2019, **375**, 121999.
27 Q. Tang, T. Lim, X.-J. Wei, Q.-Y. Wang, J.-C. Xu, L.-Y. Shen, Z.-Z. Zhu and C.-Q. Zhang, *Biomaterials*, 2020, **255**, 120138.
28 S. Homaeigohar and A. R. Boccaccini, *Acta Biomater.*, 2020, **107**, 25–49.
29 X. Chen, X. Wang, S. Wang, X. Zhang, J. Yu and C. Wang, *Mater. Sci. Eng., C*, 2020, **110**, 110624.
30 X. Zhang, D. Yao, W. Zhao, R. Zhang, B. Yu, G. Ma, Y. Li, D. Hao and F.-J. Xu, *Adv. Funct. Mater.*, 2021, **31**, 2009258.
31 J. Cao, P. Wu, Q. Cheng, C. He, Y. Chen and J. Zhou, *ACS Appl. Mater. Interfaces*, 2021, **13**, 24095–24105.
32 S. K. Das, T. Parandhaman and M. D. Dey, *Green Chem.*, 2021, **23**, 629–669.
33 R. Dong and B. Guo, *Nano Today*, 2021, **41**, 101290.
34 Z. Deng, Y. Guo, X. Zhao, T. Du, J. Zhu, Y. Xie, F. Wu, Y. Wang and M. Guan, *Gels*, 2022, **8**, 280.
35 Z. Deng, R. Yu and B. Guo, *Mater. Chem. Front.*, 2021, **5**, 2092–2123.
36 Z. Q. Li and J. J. Guan, *Polymers*, 2011, **3**, 740–761.
37 X. Zhao, Q. Lang, L. Yildirimer, Z. Y. Lin, W. Cui, N. Annabi, K. W. Ng, M. R. Dokmeci, A. M. Ghaemmaghami and A. Khademhosseini, *Adv. Healthcare Mater.*, 2016, **5**, 108–118.
38 F. Gao, Z. Xu, Q. Liang, H. Li, L. Peng, M. Wu, X. Zhao, X. Cui, C. Ruan and W. Liu, *Adv. Sci.*, 2019, **6**, 1900867.
39 T. Su, M. Zhang, Q. Zeng, W. Pan, Y. Huang, Y. Qian, W. Dong, X. Qi and J. Shen, *Bioact. Mater.*, 2021, **6**, 579–588.
40 J. Yoo, J. H. Park, Y. W. Kwon, J. J. Chung, I. C. Choi, J. J. Nam, H. S. Lee, E. Y. Jeon, K. Lee, S. H. Kim, Y. Jung and J. W. Park, *Biomater. Sci.*, 2020, **8**, 6261–6271.
41 A. L. Wollenberg, T. M. O'Shea, J. H. Kim, A. Czechanski, L. G. Reinholdt, M. V. Sofroniew and T. J. Deming, *Biomaterials*, 2018, **178**, 527–545.
42 X. Pan, S. Cheng, C. Zhang, Y. Jiao, X. Lin, W. Dong and X. Qi, *Chem. Eng. J.*, 2021, **409**, 128203.
43 S. H. Zainal, N. H. Mohd, N. Suhaili, F. H. Anuar, A. M. Lazim and R. Othaman, *J. Mater. Res. Technol.*, 2021, **10**, 935–952.
44 Q. Xu, Y. Ji, Q. Sun, Y. Fu, Y. Xu and L. Jin, *Nanomaterials*, 2019, **9**, 253.
45 J. Shin, S. Choi, J. H. Kim, J. H. Cho, Y. Jin, S. Kim, S. Min, S. K. Kim, D. Choi and S.-W. Cho, *Adv. Funct. Mater.*, 2019, **29**, 1903863.
46 H. Samadian, H. Maleki, Z. Allahyari and M. Jaymand, *Coord. Chem. Rev.*, 2020, **420**, 213432.
47 Z. J. Shi, X. Gao, M. W. Ullah, S. X. Li, Q. Wang and G. Yang, *Biomaterials*, 2016, **111**, 40–54.
48 R. Yu, M. Li, Z. Li, G. Pan, Y. Liang and B. Guo, *Adv. Healthcare Mater.*, 2022, e2102749.
49 X. Zhao, B. Guo, H. Wu, Y. Liang and P. X. Ma, *Nat. Commun.*, 2018, **9**, 2784.
50 R. Yu, H. Zhang and B. Guo, *Nano-Micro Lett.*, 2021, **14**, 1.
51 S. Pourshahrestani, E. Zeimaran, N. A. Kadri, N. Mutlu and A. R. Boccaccini, *Adv. Healthcare Mater.*, 2020, **9**, e2000905.

52 Z. Zhang, W. Jiang, X. Xie, H. Liang, H. Chen, K. Chen, Y. Zhang, W. Xu and M. Chen, *ChemistrySelect*, 2021, **6**, 12358–12382.
53 A. K. Gaharwar, N. A. Peppas and A. Khademhosseini, *Biotechnol. Bioeng.*, 2014, **111**, 441–453.
54 S. Rafieian, H. Mirzadeh, H. Mahdavi and M. E. Masoumi, *Sci. Eng. Compos. Mater.*, 2019, **26**, 154–174.
55 Z. B. Xiao, Q. X. Zhao, Y. W. Niu and D. Zhao, *Soft Matter*, 2022, **18**, 3447–3464.
56 S. R. U. Rehman, R. Augustine, A. A. Zahid, R. Ahmed, M. Tariq and A. Hasan, *Int. J. Nanomed.*, 2019, **14**, 9603–9617.
57 J. He, M. Shi, Y. Liang and B. Guo, *Chem. Eng. J.*, 2020, **394**, 124888.
58 M. Xu, Q. Li, Z. Fang, M. Jin, Q. Zeng, G. Huang, Y. G. Jia, L. Wang and Y. Chen, *Biomater. Sci.*, 2020, **8**, 6957–6968.
59 W. Shi, N. Song, Y. Huang, C. He, M. Zhang, W. Zhao and C. Zhao, *Biomacromolecules*, 2022, **23**, 889–902.
60 B. Zhang, J. He, M. Shi, Y. Liang and B. Guo, *Chem. Eng. J.*, 2020, **400**, 125994.
61 P. Li, S. Liu, X. Yang, S. Du, W. Tang, W. Cao, J. Zhou, X. Gong and X. Xing, *Chem. Eng. J.*, 2021, **403**, 126387.
62 S. Huang, H. Liu, K. Liao, Q. Hu, R. Guo and K. Deng, *ACS Appl. Mater. Interfaces*, 2020, **12**, 28952–28964.
63 Y. Lin, X. Liu, Z. Liu and Y. Xu, *Small*, 2021, **17**, e2103348.
64 A. A. Shefa, T. Sultana, M. K. Park, S. Y. Lee, J.-G. Gwon and B.-T. Lee, *Mater. Des.*, 2020, **186**, 108313.
65 H. Deng, Z. Yu, S. Chen, L. Fei, Q. Sha, N. Zhou, Z. Chen and C. Xu, *Carbohydr. Polym.*, 2020, **230**, 115565.
66 W. C. Huang, R. Ying, W. Wang, Y. Guo, Y. He, X. Mo, C. Xue and X. Mao, *Adv. Funct. Mater.*, 2020, **30**, 2000644.
67 C. Mao, Y. Xiang, X. Liu, Z. Cui, X. Yang, K. W. K. Yeung, H. Pan, X. Wang, P. K. Chu and S. Wu, *ACS Nano*, 2017, **11**, 9010–9021.
68 B. Zhang, Y. Lv, C. Yu, W. Zhang, S. Song, Y. Li, Y. Chong, J. Huang and Z. Zhang, *Biomater. Adv.*, 2022, **137**, 212869.
69 B. Ma, W. Dang, Z. Yang, J. Chang and C. Wu, *Appl. Mater. Today*, 2020, **20**, 100735.
70 M. Luo, M. Wang, W. Niu, M. Chen, W. Cheng, L. Zhang, C. Xie, Y. Wang, Y. Guo, T. Leng, X. Zhang, C. Lin and B. Lei, *Chem. Eng. J.*, 2021, **412**, 128471.
71 H. Zheng, S. Wang, F. Cheng, X. He, Z. Liu, W. Wang, L. Zhou and Q. Zhang, *Chem. Eng. J.*, 2021, **424**, 130148.
72 Y. Li, M. Han, Y. Cai, B. Jiang, Y. Zhang, B. Yuan, F. Zhou and C. Cao, *Biomater. Sci.*, 2022, **10**, 1068–1082.
73 L. Zhou, H. Zheng, Z. Liu, S. Wang, Z. Liu, F. Chen, H. Zhang, J. Kong, F. Zhou and Q. Zhang, *ACS Nano*, 2021, **15**, 2468–2480.
74 Y. Li, R. Fu, Z. Duan, C. Zhu and D. Fan, *ACS Nano*, 2022, **16**, 7486–7502.
75 X. Yang, C. Zhang, D. Deng, Y. Gu, H. Wang and Q. Zhong, *Small*, 2022, **18**, 2104368.
76 S. Zhu, Q. Dai, L. Yao, Z. Wang, Z. He, M. Li, H. Wang, Q. Li, H. Gao and X. Cao, *Composites, Part B*, 2022, **231**, 109569.
77 G. Lokhande, J. K. Carrow, T. Thakur, J. R. Xavier, M. Parani, K. J. Bayless and A. K. Gaharwar, *Acta Biomater.*, 2018, **70**, 35–47.
78 L. Han, X. Lu, K. Liu, K. Wang, L. Fang, L. T. Weng, H. Zhang, Y. Tang, F. Ren, C. Zhao, G. Sun, R. Liang and Z. Li, *ACS Nano*, 2017, **11**, 2561–2574.
79 A. Khalid, A. Madni, B. Raza, M. ul Islam, A. Hassan, F. Ahmad, H. Ali, T. Khan and F. Wahid, *Int. J. Biol. Macromol.*, 2022, **203**, 256–267.
80 Y. Liang, X. Zhao, T. Hu, Y. Han and B. Guo, *J. Colloid Interface Sci.*, 2019, **556**, 514–528.
81 M. Wang, C. G. Wang, M. Chen, M. Luo, Q. X. Chen and B. Lei, *Chem. Eng. J.*, 2022, **439**, 135629.
82 Y. Liang, B. Chen, M. Li, J. He, Z. Yin and B. Guo, *Biomacromolecules*, 2020, **21**, 1841–1852.
83 Z. Tu, M. Chen, M. Wang, Z. Shao, X. Jiang, K. Wang, Z. Yao, S. Yang, X. Zhang, W. Gao, C. Lin, B. Lei and C. Mao, *Adv. Funct. Mater.*, 2021, **31**, 2100924.
84 L. Mao, S. Hu, Y. Gao, L. Wang, W. Zhao, L. Fu, H. Cheng, L. Xia, S. Xie, W. Ye, Z. Shi and G. Yang, *Adv. Healthcare Mater.*, 2020, **9**, 2000872.
85 S. I. Basha, S. Ghosh, K. Vinothkumar, B. Ramesh, P. H. P. Kumari, K. V. M. Mohan and E. Sukumar, *Mater. Sci. Eng., C*, 2020, **111**, 110743.
86 J. Yang, Y. Chen, L. Zhao, Z. Feng, K. Peng, A. Wei, Y. Wang, Z. Tong and B. Cheng, *Composites, Part B*, 2020, **197**, 108139.
87 H. Zhang, X. Sun, J. Wang, Y. Zhang, M. Dong, T. Bu, L. Li, Y. Liu and L. Wang, *Adv. Funct. Mater.*, 2021, **31**, 2100093.
88 Z. Fan, B. Liu, J. Wang, S. Zhang, Q. Lin, P. Gong, L. Ma and S. Yang, *Adv. Funct. Mater.*, 2014, **24**, 3933–3943.
89 K. Liu, L. Dai and C. Li, *Int. J. Biol. Macromol.*, 2021, **191**, 1249–1254.
90 C. Wang, X. Jiang, H.-J. Kim, S. Zhang, X. Zhou, Y. Chen, H. Ling, Y. Xue, Z. Chen, M. Qu, L. Ren, J. Zhu, A. Libanori, Y. Zhu, H. Kang, S. Ahadian, M. R. Dokmeci, P. Servati, X. He, Z. Gu, W. Sun and A. Khademhosseini, *Biomaterials*, 2022, **285**, 121479.
91 X. Wang, Z. Wang, S. Fang, Y. Hou, X. Du, Y. Xie, Q. Xue, X. Zhou and X. Yuan, *Chem. Eng. J.*, 2021, **420**, 127589.
92 J. Li, Y. Wang, J. Yang and W. Liu, *Chem. Eng. J.*, 2021, **420**, 127638.
93 Y. Li, R. Fu, Z. Duan, C. Zhu and D. Fan, *Small*, 2022, **18**, 2200165.
94 X. Zhang, G. Zhang, H. Zhang, X. Liu, J. Shi, H. Shi, X. Yao, P. K. Chu and X. Zhang, *Chem. Eng. J.*, 2020, **382**, 122849.
95 Y. Li, R. Fu, Z. Duan, C. Zhu and D. Fan, *Bioact. Mater.*, 2022, **9**, 461–474.
96 L. Zhou, F. Chen, Z. Hou, Y. Chen and X. Luo, *Chem. Eng. J.*, 2021, **409**, 128224.
97 Y. Liang, M. Wang, Z. Zhang, G. Ren, Y. Liu, S. Wu and J. Shen, *Chem. Eng. J.*, 2019, **378**, 122043.
98 L. Siebert, E. Luna-Cerón, L. E. García-Rivera, J. Oh, J. Jang, D. A. Rosas-Gómez, M. D. Pérez-Gómez, G. Maschkowitz, H. Fickenscher, D. Oceguera-Cuevas, C. G. Holguín-León, B. Byambaa, M. A. Hussain, E. Enciso-Martínez, M. Cho, Y. Lee, N. Sobahi, A. Hasan, D. P. Orgill, Y. K. Mishra, R. Adelung, E. Lee and S. R. Shin, *Adv. Funct. Mater.*, 2021, **31**, 2007555.

99 M. Zhang, X. Qiao, W. Han, T. Jiang, F. Liu and X. Zhao, *Carbohydr. Polym.*, 2021, **266**, 118100.
100 X. Gong, M. Luo, M. Wang, W. Niu, Y. Wang and B. Lei, *Regener. Biomater.*, 2022, **9**, rbab074.
101 L. Yang, F. Liang, X. Zhang, Y. Jiang, F. Duan, L. Li and F. Ren, *Chem. Eng. J.*, 2022, **427**, 131506.
102 Z. Deng, M. Li, Y. Hu, Y. He, B. Tao, Z. Yuan, R. Wang, M. Chen, Z. Luo and K. Cai, *Chem. Eng. J.*, 2021, **420**, 129668.
103 X. Zhao, L. Chang, Y. Hu, S. Xu, Z. Liang, X. Ren, X. Mei and Z. Chen, *ACS Appl. Mater. Interfaces*, 2022, **14**, 18194–18208.
104 H. Wu, F. Li, S. Wang, J. Lu, J. Li, Y. Du, X. Sun, X. Chen, J. Gao and D. Ling, *Biomaterials*, 2018, **151**, 66–77.
105 Z. Pan, K.-R. Zhang, H.-L. Gao, Y. Zhou, B.-B. Yan, C. Yang, Z.-y. Zhang, L. Dong, S.-M. Chen, R. Xu, D.-H. Zou and S.-H. Yu, *Nano Res.*, 2020, **13**, 373–379.
106 C. Li, T. Jiang, C. Zhou, A. Jiang, C. Lu, G. Yang, J. Nie, F. Wang, X. Yang and Z. Chen, *Carbohydr. Polym.*, 2023, **299**, 120198.
107 W. Niu, M. Chen, Y. Guo, M. Wang, M. Luo, W. Cheng, Y. Wang and B. Lei, *ACS Nano*, 2021, **15**, 14323–14337.
108 M. Long, Q. Liu, D. Wang, J. Wang, Y. Zhang, A. Tang, N. Liu, B. Bui, W. Chen and H. Yang, *Mater. Today Adv.*, 2021, **12**, 100190.
109 K. Haraguchi, T. Takehisa and S. Fan, *Macromolecules*, 2002, **35**, 10162–10171.
110 Z. Deng, Y. Guo, X. Zhao, P. X. Ma and B. Guo, *Chem. Mater.*, 2018, **30**, 1729–1742.
111 Z. Deng, T. Hu, Q. Lei, J. He, P. X. Ma and B. Guo, *ACS Appl. Mater. Interfaces*, 2019, **11**, 6796–6808.
112 Z. Deng, H. Wang, P. X. Ma and B. Guo, *Nanoscale*, 2020, **12**, 1224–1246.
113 B. Grigoryan, S. J. Paulsen, D. C. Corbett, D. W. Sazer, C. L. Fortin, A. J. Zaita, P. T. Greenfield, N. J. Calafat, J. P. Gounley, A. H. Ta, F. Johansson, A. Randles, J. E. Rosenkrantz, J. D. Louis-Rosenberg, P. A. Galie, K. R. Stevens and J. S. Miller, *Science*, 2019, **364**, 458–464.
114 H. Yi, M. Seong, K. Sun, I. Hwang, K. Lee, C. Cha, T.-i. Kim and H. E. Jeong, *Adv. Funct. Mater.*, 2018, **28**, 1706498.
115 K. Škrlová, K. Malachová, A. Muñoz-Bonilla, D. Měřinská, Z. Rybková, M. Fernández-García and D. Plachá, *Nanomaterials*, 2019, **9**, 1548.
116 Z. Deng, Y. Guo, X. Zhao, L. Li, R. Dong, B. Guo and P. X. Ma, *Acta Biomater.*, 2016, **46**, 234–244.
117 P. Lavrador, M. R. Esteves, V. M. Gaspar and J. F. Mano, *Adv. Funct. Mater.*, 2021, **31**, 2005941.
118 W. Peng, D. Li, K. L. Dai, Y. X. Wang, P. Song, H. R. Li, P. Tang, Z. Y. Zhang, Z. Y. Li, Y. C. Zhou and C. C. Zhou, *Int. J. Biol. Macromol.*, 2022, **208**, 400–408.
119 X. Zhao, Z. Zhang, J. Luo, Z. Wu, Z. Yang, S. Zhou, Y. Tu, Y. Huang, Y. Han and B. Guo, *Appl. Mater. Today*, 2022, **26**, 101365.
120 T. Hu, M. Shi, X. Zhao, Y. Liang, L. Bi, Z. Zhang, S. Liu, B. Chen, X. Duan and B. Guo, *Chem. Eng. J.*, 2022, **428**, 131017.
121 M. Li, Z. Zhang, Y. Liang, J. He and B. Guo, *ACS Appl. Mater. Interfaces*, 2020, **12**, 35856–35872.
122 W. Huang, Y. Wang, Y. Chen, Y. Zhao, Q. Zhang, X. Zheng, L. Chen and L. Zhang, *Adv. Healthcare Mater.*, 2016, **5**, 2813–2822.
123 Y. Ma, J. Yao, Q. Liu, T. Han, J. Zhao, X. Ma, Y. Tong, G. Jin, K. Qu, B. Li and F. Xu, *Adv. Funct. Mater.*, 2020, **30**, 2001820.
124 X. Xia, X. Xu, B. Wang, D. Zhou, W. Zhang, X. Xie, H. Lai, J. Xue, A. Rai, Z. Li, X. Peng, P. Zhao, L. Bian and P. W.-Y. Chiu, *Adv. Funct. Mater.*, 2022, **32**, 2109332.
125 Y. Huang, X. Zhao, C. Wang, J. Chen, Y. Liang, Z. Li, Y. Han and B. Guo, *Chem. Eng. J.*, 2022, **427**, 131977.
126 Y. Hong, F. Zhou, Y. Hua, X. Zhang, C. Ni, D. Pan, Y. Zhang, D. Jiang, L. Yang, Q. Lin, Y. Zou, D. Yu, D. E. Arnot, X. Zou, L. Zhu, S. Zhang and H. Ouyang, *Nat. Commun.*, 2019, **10**, 2060.
127 E. E. Leonhardt, N. Kang, M. A. Hamad, K. L. Wooley and M. Elsabahy, *Nat. Commun.*, 2019, **10**, 2307.
128 Z. Qiao, X. Lv, S. He, S. Bai, X. Liu, L. Hou, J. He, D. Tong, R. Ruan, J. Zhang, J. Ding and H. Yang, *Bioact. Mater.*, 2021, **6**, 2829–2840.
129 S. An, E. J. Jeon, J. Jeon and S.-W. Cho, *Mater. Horiz.*, 2019, **6**, 1169–1178.
130 Y. Huang, X. Zhao, Z. Zhang, Y. Liang, Z. Yin, B. Chen, L. Bai, Y. Han and B. Guo, *Chem. Mater.*, 2020, **32**, 6595–6610.
131 Z. Chen, H. Wu, H. Wang, D. Zaldivar-Silva, L. Agüero, Y. Liu, Z. Zhang, Y. Yin, B. Qiu, J. Zhao, X. Lu and S. Wang, *Mater. Sci. Eng., C*, 2021, **129**, 112422.
132 W. Huang, S. Cheng, X. Wang, Y. Zhang, L. Chen and L. Zhang, *Adv. Funct. Mater.*, 2021, **31**, 2009189.
133 H. Lee, S. M. Dellatore, W. M. Miller and P. B. Messersmith, *Science*, 2007, **318**, 426–430.
134 S. Li, S. Dong, W. Xu, S. Tu, L. Yan, C. Zhao, J. Ding and X. Chen, *Adv. Sci.*, 2018, **5**, 1700527.
135 Y. Liang, Y. Liang, H. Zhang and B. Guo, *Asian J. Pharm. Sci.*, 2022, **17**, 353–384.
136 Z. Yang, R. Huang, B. Zheng, W. Guo, C. Li, W. He, Y. Wei, Y. Du, H. Wang, D. Wu and H. Wang, *Adv. Sci.*, 2021, **8**, 2003627.
137 D. Gan, T. Xu, W. Xing, X. Ge, L. Fang, K. Wang, F. Ren and X. Lu, *Adv. Funct. Mater.*, 2019, **29**, 1805964.
138 K. Wang, J. Wang, L. Li, L. Xu, N. Feng, Y. Wang, X. Fei, J. Tian and Y. Li, *Chem. Eng. J.*, 2019, **372**, 216–225.
139 W. Liu, W. Ou-Yang, C. Zhang, Q. Wang, X. Pan, P. Huang, C. Zhang, Y. Li, D. Kong and W. Wang, *ACS Nano*, 2020, **14**, 12905–12917.
140 C. Shuai, G. Liu, Y. Yang, F. Qi, S. Peng, W. Yang, C. He, G. Wang and G. Qian, *Nano Energy*, 2020, **74**, 104825.
141 X. Qu, H. Yang, B. Jia, Z. Yu, Y. Zheng and K. Dai, *Acta Biomater.*, 2020, **117**, 400–417.
142 Q. Xin, H. Shah, A. Nawaz, W. Xie, M. Z. Akram, A. Batool, L. Tian, S. U. Jan, R. Boddula, B. Guo, Q. Liu and J. R. Gong, *Adv. Mater.*, 2019, **31**, 1804838.
143 Y. Fu, L. Yang, J. Zhang, J. Hu, G. Duan, X. Liu, Y. Li and Z. Gu, *Mater. Horiz.*, 2021, **8**, 1618–1633.
144 X. Zhang, C. Zhang, Y. Yang, H. Zhang, X. Huang, R. Hang and X. Yao, *Chem. Eng. J.*, 2019, **374**, 596–604.

145 J. Sun, L. Song, Y. Fan, L. Tian, S. Luan, S. Niu, L. Ren, W. Ming and J. Zhao, *ACS Appl. Mater. Interfaces*, 2019, **11**, 26581–26589.
146 J. Chi, X. Zhang, C. Chen, C. Shao, Y. Zhao and Y. Wang, *Bioact. Mater.*, 2020, **5**, 253–259.
147 J. Li, S. Yuan, J. Zhu and B. Van der Bruggen, *Chem. Eng. J.*, 2019, **373**, 275–284.
148 L. Ren, G. He, Y. Zhou, J. Dai, W. Miao, C. Ouyang, J. Liu and G. Chen, *Biomater. Sci.*, 2022, **10**, 3174–3187.
149 M. Wang, C. G. Wang, M. Chen, Y. W. Xi, W. Cheng, C. Mao, T. Z. Xu, X. X. Zhang, C. Lin, W. Y. Gao, Y. Guo and B. Lei, *ACS Nano*, 2019, **13**, 10279–10293.
150 Y. Tang, X. Lan, C. Liang, Z. Zhong, R. Xie, Y. Zhou, X. Miao, H. Wang and W. Wang, *Carbohydr. Polym.*, 2019, **219**, 113–120.
151 M. Ghodrati, M. R. Farahpour and H. Hamishehkar, *Colloids Surf., A*, 2019, **564**, 161–169.
152 M. Luo, K. Shaitan, X. Qu, A. P. Bonartsev and B. Lei, *Appl. Mater. Today*, 2022, **26**, 101304.
153 P. Wang, S. Huang, Z. Hu, W. Yang, Y. Lan, J. Zhu, A. Hancharou, R. Guo and B. Tang, *Acta Biomater.*, 2019, **100**, 191–201.
154 N. Lohmann, L. Schirmer, P. Atallah, E. Wandel, R. A. Ferrer, C. Werner, J. C. Simon, S. Franz and U. Freudenberg, *Sci. Transl. Med.*, 2017, **9**, eaai9044.
155 C. Dunnill, T. Patton, J. Brennan, J. Barrett, M. Dryden, J. Cooke, D. Leaper and N. T. Georgopoulos, *Int. Wound J.*, 2017, **14**, 89–96.
156 Z. Xu, G. Liu, J. Huang and J. Wu, *ACS Appl. Mater. Interfaces*, 2022, **14**, 7680–7689.
157 N. Gupta, B. F. Lin, L. M. Campos, M. D. Dimitriou, S. T. Hikita, N. D. Treat, M. V. Tirrell, D. O. Clegg, E. J. Kramer and C. J. Hawker, *Nat. Chem.*, 2010, **2**, 138–145.
158 A. Singh, S. Halder, S. Chumber, M. C. Misra, L. K. Sharma, A. Srivastava and G. R. Menon, *Asian J. Surg.*, 2004, **27**, 326–332.
159 V. J. Jones, *Int. Wound J.*, 2006, **3**, 79–88.
160 D. B. Hom, G. Adams, M. Koreis and R. Maisel, *Otolaryngol.–Head Neck Surg.*, 1999, **121**, 591–598.
161 A. Z. K. MD, N. T. MD and M. A. MD, *J. Wound Care*, 2005, **14**, 42–44.
162 J. Xiao, Y. J. Zhou, M. Q. Ye, Y. An, K. N. Wang, Q. J. Wu, L. W. Song, J. W. Zhang, H. C. He, Q. W. Zhang and J. Wu, *Adv. Healthcare Mater.*, 2021, **10**, 2001591.
163 G. D. Winter, *Nature*, 1962, **193**, 293–294.
164 J. P. E. Junker, R. A. Kamel, E. J. Caterson and E. Eriksson, *Adv. Wound Care*, 2013, **2**, 348–356.
165 S. Metzger, *Home Healthc Now*, 2004, **22**, 586–590.
166 S. Koosehgol, M. Ebrahimian-Hosseinabadi, M. Alizadeh and A. Zamanian, *Mater. Sci. Eng., C*, 2017, **79**, 66–75.
167 S. Park and K. M. Park, *Biomaterials*, 2018, **182**, 234–244.
168 A. S. Pandit and D. S. Feldman, *Wound Repair Regen.*, 1994, **2**, 130–137.
169 H. Ma, Q. Zhou, J. Chang and C. Wu, *ACS Nano*, 2019, **13**, 4302–4311.
170 S. O. Blacklow, J. Li, B. R. Freedman, M. Zeidi, C. Chen and D. J. Mooney, *Sci. Adv.*, 2019, **5**, eaaw3963.
171 Y. Zhu, J. Zhang, J. Song, J. Yang, Z. Du, W. Zhao, H. Guo, C. Wen, Q. Li, X. Sui and L. Zhang, *Adv. Funct. Mater.*, 2020, **30**, 1905493.
172 M. Li, Y. Liang, J. He, H. Zhang and B. Guo, *Chem. Mater.*, 2020, **32**, 9937–9953.
173 D. Roy, W. L. A. Brooks and B. S. Sumerlin, *Chem. Soc. Rev.*, 2013, **42**, 7214–7243.
174 H. S. Jung, P. Verwilst, A. Sharma, J. Shin, J. L. Sessler and J. S. Kim, *Chem. Soc. Rev.*, 2018, **47**, 2280–2297.
175 D. Zhi, T. Yang, J. O'Hagan, S. Zhang and R. F. Donnelly, *J. Controlled Release*, 2020, **325**, 52–71.
176 J. Chen, C. Ning, Z. Zhou, P. Yu, Y. Zhu, G. Tan and C. Mao, *Prog. Mater. Sci.*, 2019, **99**, 1–26.
177 C. Tong, X. Zhong, Y. Yang, X. Liu, G. Zhong, C. Xiao, B. Liu, W. Wang and X. Yang, *Biomaterials*, 2020, **243**, 119936.
178 Y. Liang, M. Li, Y. Yang, L. Qiao, H. Xu and B. Guo, *ACS Nano*, 2022, **16**, 3194–3207.
179 G. Kocak, C. Tuncer and V. Bütün, *Polym. Chem.*, 2017, **8**, 144–176.
180 L. Wang, Y. Wu, B. Guo and P. X. Ma, *ACS Nano*, 2015, **9**, 9167–9179.
181 Y. Wu, L. Wang, B. Guo and P. X. Ma, *ACS Nano*, 2017, **11**, 5646–5659.
182 T. Chen, Y. Chen, H. U. Rehman, Z. Chen, Z. Yang, M. Wang, H. Li and H. Liu, *ACS Appl. Mater. Interfaces*, 2018, **10**, 33523–33531.
183 M. Chen, J. Tian, Y. Liu, H. Cao, R. Li, J. Wang, J. Wu and Q. Zhang, *Chem. Eng. J.*, 2019, **373**, 413–424.
184 A. Zhang, Y. Liu, D. Qin, M. Sun, T. Wang and X. Chen, *Int. J. Biol. Macromol.*, 2020, **164**, 2108–2123.
185 D. L. Taylor and M. in het Panhuis, *Adv. Mater.*, 2016, **28**, 9060–9093.
186 T. W. Ebbesen, *Annu. Rev. Mater. Sci.*, 1994, **24**, 235–264.
187 R. C. Haddon, *Acc. Chem. Res.*, 2002, **35**, 997.
188 H. Dai, *Surf. Sci.*, 2002, **500**, 218–241.
189 L. Feng and Z. Liu, *Nanomedicine*, 2011, **6**, 317–324.
190 A. K. Geim, *Science*, 2009, **324**, 1530–1534.
191 X. Qi, Y. Huang, S. You, Y. Xiang, E. Cai, R. Mao, W. Pan, X. Tong, W. Dong, F. Ye and J. Shen, *Adv. Sci.*, 2022, **9**, 2106015.
192 V. R. Askary, N. A. Jahan, A. Sabbagh, F. S. Jahani, N. Dourandish and A. R. K. Kamachali, *Clin. Biochem.*, 2011, **44**, S323–S324.
193 B. Li, H. M. Wen, Y. J. Cui, W. Zhou, G. D. Qian and B. L. Chen, *Adv. Mater.*, 2016, **28**, 8819–8860.
194 F. Hu, S. S. Xia, Y. He, Z. L. Huang, H. Ke and J. Z. Liao, *Colloids Surf., B*, 2022, **213**, 112425.
195 Y. Chen, J. Cai, D. Liu, S. Liu, D. Lei, L. Zheng, Q. Wei and M. Gao, *Regener. Biomater.*, 2022, **9**, rbac019.
196 L. Q. Fu, X. Y. Chen, M. H. Cai, X. H. Tao, Y. B. Fan and X. Z. Mou, *Front. Bioeng. Biotechnol.*, 2020, **8**, 576348.
197 H. Wang, Z. Xu, Q. Li and J. Wu, *Engineered Regeneration*, 2021, **2**, 137–153.
198 M. Naguib, M. Kurtoglu, V. Presser, J. Lu, J. J. Niu, M. Heon, L. Hultman, Y. Gogotsi and M. W. Barsoum, *Adv. Mater.*, 2011, **23**, 4248–4253.
199 Y. Gogotsi and B. Anasori, *ACS Nano*, 2019, **13**, 8491–8494.

200 B. Song and Y. He, *Nano Today*, 2019, **26**, 149–163.
201 F. Peng, Y. Su, Y. Zhong, C. Fan, S.-T. Lee and Y. He, *Acc. Chem. Res.*, 2014, **47**, 612–623.
202 M. Mesa and N. Y. Becerra, *Int. J. Biomater.*, 2021, **2021**, 6857204.
203 C. Wang, H. Niu, X. Ma, H. Hong, Y. Yuan and C. Liu, *ACS Appl. Mater. Interfaces*, 2019, **11**, 34595–34608.
204 A. M. Villalba-Rodriguez, S. Martinez-Gonzalez, J. E. Sosa-Hernandez, R. Parra-Saldivar, M. Bilal and H. M. N. Iqbal, *Gels*, 2021, **7**, 59.
205 A. N. Ordeghan, D. Khayatan, M. R. Saki, M. Alam, K. Abbasi, H. Shirvani, M. Yazdanian, R. S. Soufdoost, H. T. Raad, A. Karami and H. Tebyaniyan, *Adv. Mater. Sci. Eng.*, 2022, **2022**, 9222003.
206 L. F. Fan, X. Wang and D. C. Wu, *Chin. J. Chem.*, 2021, **39**, 757–774.
207 C. Yang, H. Huang, S. Fan, C. Yang, Y. Chen, B. Yu, W. Li and J. Liao, *Adv. Mater. Technol*, 2021, **6**, 2001012.
208 U. Pantulap, M. Arango-Ospina and A. R. Boccaccini, *J. Mater. Sci.: Mater. Med.*, 2022, **33**, 3.
209 L. Zhou, Y. Xi, Y. Xue, M. Wang, Y. Liu, Y. Guo and B. Lei, *Adv. Funct. Mater.*, 2019, **29**, 1806883.
210 Y. Li, T. Xu, Z. Tu, W. Dai, Y. Xue, C. Tang, W. Gao, C. Mao, B. Lei and C. Lin, *Theranostics*, 2020, **10**, 4929–4943.
211 M. Chen, D. D. Winston, M. Wang, W. Niu, W. Cheng, Y. Guo, Y. Wang, M. Luo, C. Xie, T. Leng, X. Qu and B. Lei, *Mater. Today*, 2022, **53**, 27–40.
212 W. Niu, Y. Guo, Y. Xue, M. Wang, M. Chen, D. D. Winston, W. Cheng and B. Lei, *Nano Today*, 2021, **38**, 101137.